MATERIAL FLOW IN SUNKEN FORGING-DIES

YASUO KASUGA, SHIGEAKI TSUTSUMI, and HIROYUKI SAIKI

Department of Mechanical Engineering

(Received October 31, 1973)

In this paper, plane strain and axi-symmetric plastic flows in the forging dies which consist of horizontal and vertical passages connected with corner fillets are referred to. In the experiment, a plasticine model material has been shaped into the component with ribs or a boss. The upper-bound technique is applied to explain the patterns of material flow which were observed through experiment.

In the region joining the rim or boss with the web and the flash, five typical modes of deformation appear in a certain sequence which is mainly controlled by the geometry of the die passages, width-height ratio of the flash and height-width ratio of the joining region, and by the frictional shear stress acting on the flash land. According to the deformation mode, the filling-in velocities and the forming loads appear to have much differences.

In order to improve the die filling with less energy consumption, it becomes necessary to adjust the forging parameters so that in a process the optimum sequence of deformation modes can be attained. By noticing the transitional conditions of deformation mode which are clarified by experiment and predicted also by theory, an approach to the optimization of forging parameters which were done empirically so far have been systematized.

1. Introduction

In the field of metal working process, die-forging is regarded as one of the important methods to produce many engineering components. However, general designing principle of forgings and the forging-dies utilized have not been established consistently so that the determination of forging parameters still relies much on empirical methods.

Recently, high-velocity forgings in hot state have been introduced by many practical staffs in order to forge metals either of poor forgeability or of high flow strength. In this kind of single-blow forging processes, it becomes essential in design problem how to choose die and billet dimensions as to prevent forging defects such as the overlap, the cold shut, the extrusion defect, the flow-through defect and so on.

When the specialities of a closed die-forging process are considered, it will be easy to see that the material flow is in an unsteady state and is closely connected with the particular geometry of the forging. Therefore, it has been a difficult matter to treat the material flow consistently.

In many papers hitherto published on the die-forging the forming resistance or the load necessary for working is seemed to be the main event of treaties. These works have made possible to predict the forging load and stress through the analytical methods plausible. However, it is only in recent years that the investigations on the material flow and the filling-in phenomena in closed die forging appear.

J. Stöter has made a study of hot forging processes in which a central bosses were produced under the various forming conditions. On the basis of the experimental results, he recommended for the boss formation that a stubby shaped blank should be used to form a central boss in the upper die when a low speed press is used. And it has been also found that flash-land width is so chosen that the final width-height ratio of the flash comes to 5. It has been also shown by K. Vieregge that the optimum thickness of the flash and final width height ratio of the flash depend on the size and the shape of the forgings. H. Takahashi *et al.* and H. Takei *et al.* analysed the boss formation mechanism. Their results have given a useful guide to practical problems.

H. Rauhause *et al.* and A. M. Sabroff *et al.* have pointed out the interesting relation between forging defects and the material behaviour in the die cavities. In spite of these leading works, the general aspect of the material flow in sunken forging-die as yet appears to be scarcely available.

In view of the material flow, the die impressions may be said to consist of the horizontal and vertical or inclined passages which are connected with fillets having two different functions for the flow as shown in Fig. 1 (a) and (b). Under a condition of axial symmetry the material which laid on a relevant portion of the die cavity is forced to flow centrifugally or centripetally and then to part into several directions taken by the passages. Consequently, geometry of deformation shown in Fig. 1 (c) may be considered as a typical model where the specialities of the material flow in the closed-die are expressed fully (Arrows represent segments of flow lines).

In the present investigation, two-dimentional model forging dies are utilized in order to clarify the prototypes of the deformation which involves parting of the material flow into several directions. Furthermore, axi-symmetric models are also tested in which the components consisting of ribs or a rim, a boss and a web are shaped using the relevant model dies. As a result, five typical modes of deformation have been observed in the regions joining the rib and the web, which are regarded as prototypes of the rim formation under the plane strain and axi-symmetric conditions. In the process, these typical deformation modes succesively occur in accordance with the geometry governing the die cavity and the material. It has been proved that the sequence of these deformation modes are very important for improving the die-filling.

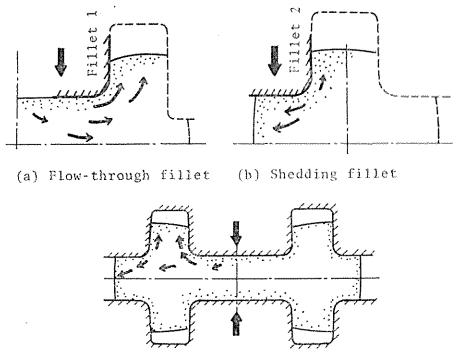

(a) Flow-through fillet (b) Shedding fillet

(c) Material flow controlled by the combination of fillets (a) and (b).

FIG. 1. Movement of material along the fillet.

This work has aimed at the establishment of a designing principle of forging-die as well as relating optimum size of the blank. Therefore, the present study purports:

(1) to find out several kinds of typical deformation modes and to cofirm critical conditions under one of which the deformation mode in a process changes

to another;

(2) to clarify the influence of the geometries of die and material on the conditions;

(3) to predict the necessary forging load and the changing point of deformation mode using the upper-bound methods;

(4) to establish a designing principle of forging-die as well as to determine the relating optimum size of the blank utilizing the results obtained in the items (1) ~ (3), and

(5) to systematize mechanisms of the rim or boss formation under the plane strain and the axi-symmetric conditions.

2. Model material

It is very difficult to use practical metal in hot state in order to observe continuously the material flow in the die. Up to this time many investigators have used model material such as lead, tellur-lead, mixture of waxes or plasticine for this purpose.

Attempts have been made by A. P. Green, by P. M. Cook and by Y. Awano to examine the mechanical properties which a plasticine possesses for such experimental application. It has been clarified by them that the flow patterns and the distribution of strain rate are similar in both the plasticine and an ideal metal or a mild steel in hot state. So, in this experiment, a plasticine was utilized as a model material under the condition of exactly controlled temperature, (20 ± 1)°C and speed $\dot{\varepsilon}=0.003$/s.

The stress-strain curves of a plasticine obtained by uniaxial compression are shown in Fig. 2 (a) and (b). The flow stress shows a strong temperature dependence as shown in Fig. 2 (a). At low temperature there is a sharp bend similar to that of a hardened metal or an ideally plastic metal. At high temperature, however, the tendency of the curve is similar to that of an annealed metal.

In a model material such as a plasticine whose flow stress sensitively depends on temperature the characteristics of the flow stress may be affected by the variation of strain rate. The flow stress curves at various strain rates are shown in Fig. 2 (b). The difference of flow stress at $\varepsilon=0.25$ attains even approximately 0.42 kg/cm^2. A tendency of even work-soften

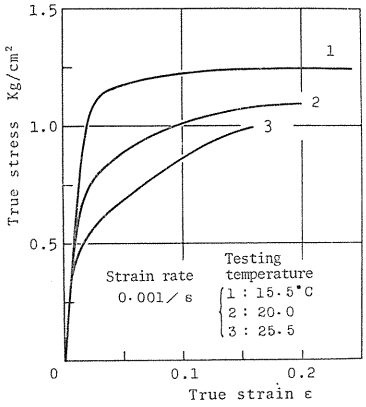

(a) Effect of the testing temperature (Lot No.1.)

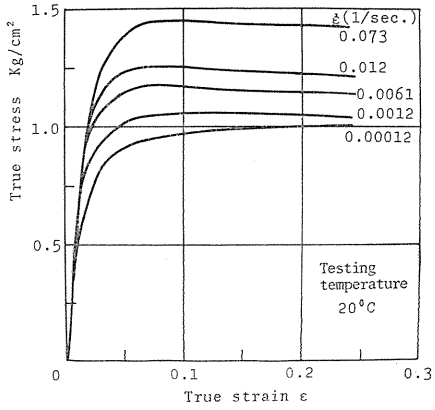

(b) Effect of the strain rate. (Lot No.2.)

FIG. 2. Stress-strain curves of the plasticine model material in compression tests.

ing seems to appear at $\dot{\varepsilon}=0.02/s$.

For previously forming plasticine into a blank shape and preforming the experimental deformation process, a 10 ton universal testing machine was utilized at the constant temperature. First, about 50 lb. white plasticine was mixed together at a time to prepare a homogeneous mass, and it was divided into small masses. After kneading them carefully by hand to eliminate air bubble, a piece of the block was shaped into a blank having desired form by metal dies. Before the experiment, blanks are kept at a constant temperature of 20°C for a whole day.

3. Representation of the geometry in relation to the forging

3.1. Flow model and observation of material flow

On the basis of the section geometry as shown in Fig. 1 (c), the compound material flow will be examined by two types of model die whose schematic diagrams are shown in Fig. 3. As will be seen, these model dies are different from practical die-form in the neglect of corner radii and drafts. However, it was

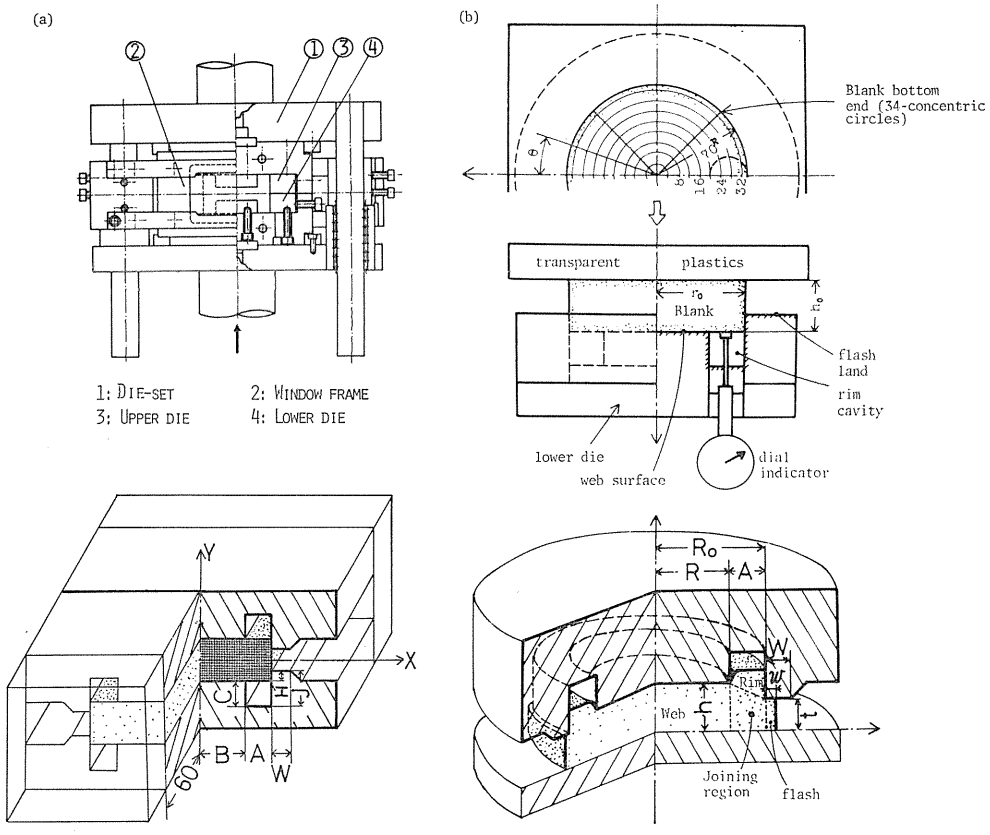

FIG. 3. Schematic illustration of two types of model forging die
(a) Plane strain condition
(b) Condition of axial symmetry: The material beneath the web flows centrifugally.

expected that prototypes of the material flow could be observed in these types of dies.

These model dies are composed of sharp cornered steel blocks or disks whose surfaces are finished smoothly by grinding until a surface roughness of $R_{max}=1.6$ μm is obtained. In order to observe the material flow during the process, some parts of the die-assembly are accommodated to be replaced by the transparent plastics.

In the case of plane strain shown in Fig. 3 (a), the material flow in xy-plane can be easily observed by deformation of the grid which was printed previously on the sectional xy-plane of the blank material. Because the sectional plane lays in the middle of z-direction, the non-disturbed deformation figures could be photographed by wholly removing the front half of the die-material assembly. On the other hand, in axisymmetric conditions of Fig. 3 (b) where the material beneath the web face of the die flows centrifugally, observation of the flow patterns on the central plane or rz-plane will be difficult because of the distorsion of the sectional plane. Therefore, as will be seen in the figure, the concentric circles printed on the bottom surface of the blank were successively photographed, while, the displacement of the rim tip was measured by a dial-indicator.

3.2. *Parameters representing the geometry*

In order to specify the section geometry encountered, some specific values or the ratios of dimensions should be mentioned. In this paper, the web half width B in plane strain and the web radius R in axial symmetry were employed as a referring dimensional scale. The sectional shape of the die-impression as shown in Fig. 4 (a) will be represented by giving the ratio of the rim width and the web-half A/B or A/R, the ratio of the web thickness to the web width H/B or H/R and that of the rim height to its width J/A.

For a process where the material flows over flash lands, width of the flash land W should be also taken into account.

Once the above mentioned parameters for the die have been given, volume of the material which can fill just the closed cavity of the dies without any excess or deficiency will be written as below.

$$V_{io}=4(AJ+BH)=4B^2\{(A/B)^2(J/A)+H/B\}$$
$$=F_{io} \text{ (sectional area)}$$

for the unit depth of plane strain condition,

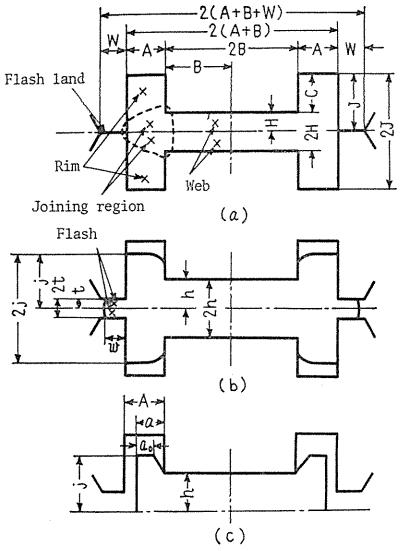

FIG. 4. Shape parameters of closed-die forging.

$$V_{io}=2\pi R^3\{(A/R)^2(J/A)(2+A/R)+H/R\} \quad \text{for axial symmetry.}$$

This may be said to be the necessary minimum volume of the blank. For a

condition of die filling in which the die engravings are filled up and the flashes having a thickness of $2t$ take place, volume of the forging after trimming may be written as

$$V_i = F_i = F_{io} + 4t(A+B) \quad \text{for plane strain,}$$
$$V_i = V_{io} + 2\pi \cdot (A+R)^2 t \quad \text{for axial symmetry.}$$

In this case, if the material of $4f$ or $2\pi f$ flows through the flash lands to the gutters, the volume of the blank to be prepared must be

$$V_a = F_a = 4\{(AJ+BH)+t(A+B+W)+f\} = 4h_0b_0 \quad \text{for plane strain,}$$
$$V_a = 2\pi\{AJ(A+2R)+R^2H+t(A+R+W)^2+f\} = 2\pi r_0^2 h_0$$
$$\text{for axial symmetry.}$$

In order to specify the section geometry of the blank, it will be necessary to give the ratio h_0/b_0 or h_0/r_0, b_0/B or r_0/R and the scale dimension B or R. In process, when the web thickness is reduced to $2h$, the possible half-thickness of the flash will be given by $t=h-H$, so that the width-height ratio of the flash may be $w/2t$ or simply w/t. Then the volume of flash $V_f(t)$ in a process is equal to $4wt$ or $2\pi t\{(A+R+w)^2-(A+R)^2\}$. See Fig. 4 (b).

Utilizing the parameters specified above, the following induced parameters can be written:

Percentage of surplus material:	$\phi = (V_a - V_i)/V_i = (V_a/V_i) - 1$	(3.1)
	$\phi_0 = (V_a - V_{io})/V_{io} = (V_a/V_{io}) - 1$	(3.2)
Efficacious material:	$Y = V_i/V_a = 1/(1+\phi)$	(3.3)
Degree of die closure:	$\delta_c = (h_0 - h)/(h_0 - H) = 1 - t/(h_0 - H)$	(3.4)
Relative volume of the flash:	$\varphi = V_f(t)/V_a = Y \cdot V_f(t)/V_i$	(3.5)

4. Geometry of deformation in plane strain condition

4.1. Typified modes of deformation

In order to specify the experimental conditions, some apriori grants would be still required for defining the values of forging parameters mentioned above.

In this investigation, aiming at a finished component which is composed of the web and the rim having equal and uniform thicknesses, A/B of 0.6 has been chosen as a fundamental ratio and $A/H=(A/B)/(H/B)=0.6/0.3=2$ so that A/H is fixed at 2.

Table 1 gives the value of the variables in the test. In this test, the tools having the ratios and dimensions of $A/B=0.6$, $H/B=0.3$, $J/A=1.5$, $2B=50$ mm and $W=30$ mm were regarded as those of the fundamental form. See Table 1 above.

At first, 4 kinds of blanks listed in Table 1-group II were formed by the tools with fundamental dimensions. Photographs in Fig. 5 show the states of distortion of the square grid originally printed on the sectional plane.

It is observed that when the width of blank material $2b_0$ is smaller than $2(A+B)$, the deformation of material in early stage of the process is similar to that of simple upsetting of a slab between parallel anvils. So, it might be said

TABLE 1. Values of the experimental variables

Shape parameters in the die					
	Width ratio of the rim and the web A/B	Heigh-width ratio of the web H/B	Height-width ratio of the rim J/A	Web width $2B$ mm	Flash land width W mm
Fundamental value	0.6	0.3	1.5	50	30
Altered value	0.4, 0.8	0.1, 0.2			10.5, 5.5, 1.2

Shape parameters of blank				
Group	Percentage of surplus material % $\psi_0=(F_a/F_{io})-1$	Height-width ratio h_0/b_0	Width ratio of blank and the web b_0/B ($2B=50$ mm)	Remarks
I	about 26	0.415	1.6	Standard
		0.534	1.4	Altered
		0.731	1.2	Altered
		1.054	1.0	Altered
II	6.8	0.350	1.6	Altered
	16.2	0.381	1.6	Altered
	26.4	0.415	1.6	Standard
	36.1	0.446	1.6	Altered
	44.2	0.472	1.6	Altered
III	7.1	0.341	1.8	Altered
	16.1	0.381	1.6	Altered
	30.7	0.438	1.4	Altered

that the flow peculiar to this kind of die forging could not take place until the material reached the entrance of flash lands. Hence, in the beginning the observation was confined to the case when the blank width $2b_0$ equals to $2(A+B)$, and this condition is shown in (a) of Fig. 5. In this case, the detailed deformation patterns in process are shown in Fig. 6. The right hand halves of the figures show the distorted grids and the left hand halves their deformation schemes. In the left half illustrations, the square grids represent the region where the deformation has not taken place, the inclined solid lines represent the portions of high strain rate, the dotted regions correspond to the plastic zones and the white regions to the rigid zones which translate bodily under these relevant configurations.

As will be seen in Fig. (i) ~ (v), throughout a process, the deformation pattern of material between the web faces (region 11'2'2) is similar to that of the plane strain indentation of flat anvils into a rectangular blank.

The condition is somewhat peculiar in the region of rims and in the joining region because the sunken depth H of the web affects the flow. See Fig. 4 (a). In fact, the region 578 in Fig. 6 (i) is able to move upward along the side wall 45 as if it were a chip in cutting with a shear plane 57. In the bud of flash portion 56, a similar deformation is observed according to the scraping action of the flash land. As the filling of the rim goes on, shear plane 57 changes its direction to 52. Consequently, material in the rim and the joining region can move as a rigid body as shown in Fig. 6 (ii). In these two stages the material contained in the rim rises according to a mechanism like chip removal in the cutting and so the material in the joining region can move as a rigid body.

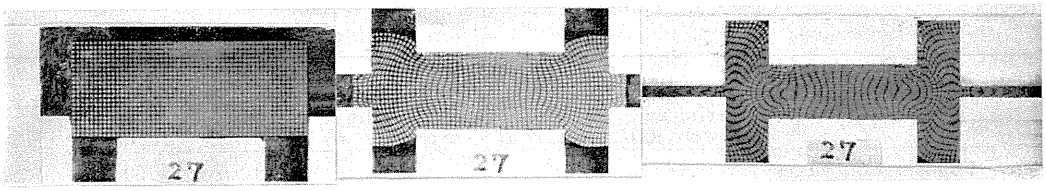

(a) Blank dimension $h_0/b_0=0.415$; $b_0=80$ mm, $h_0=33.2$ mm, Die-stroke (Degree of die-closure) $s=0$ mm ($\delta c=0\%$), $s=7.19$ mm ($\delta c=39.6\%$), $s=14.3$ mm ($\delta c=78.9\%$)

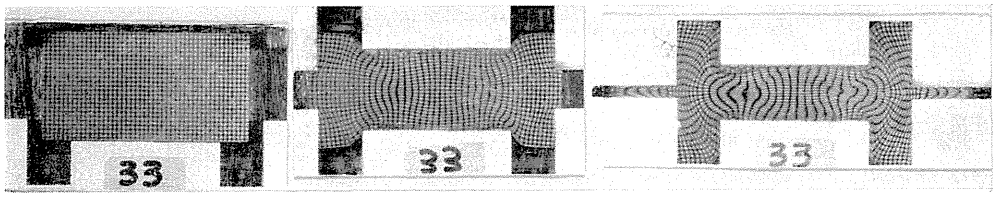

(b) Blank dimension $h_0/b_0=0.534$; $b_0=70$ mm, $h_0=37.4$ mm $s=0$ ($\delta c=0$), $s=10.43$ ($\delta c=46.5$), $s=18.53$ ($\delta c=82.8$)

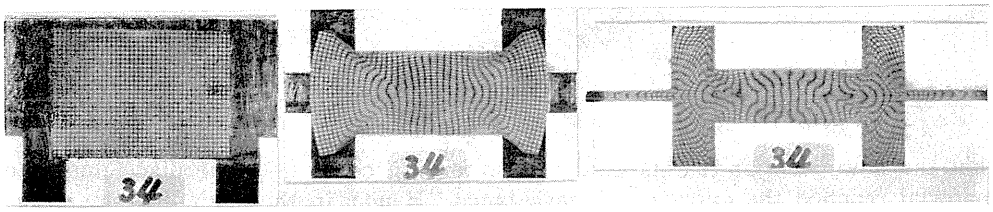

(c) Blank dimension $h_0/b_0=0.731$; $b_0=60$ mm, $h_0=43.9$ mm $s=0$ ($\delta c=0$), $s=12.96$ ($\delta c=45.8$), $s=24.38$ ($\delta c=86.0$)

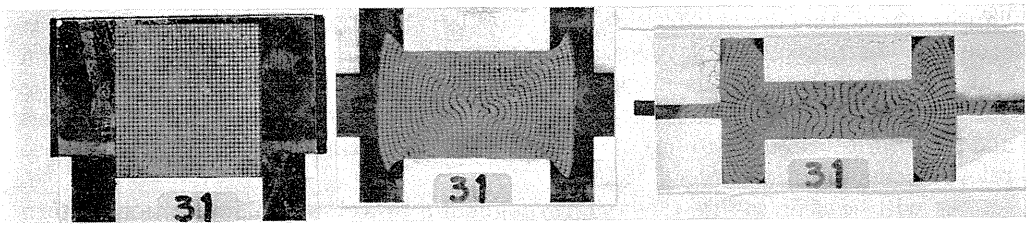

(d) Blank dimension $h_0/b_0=1.054$; $b_0=50$ mm, $h_0=52.7$ mm $s=0$ ($\delta c=0$) $s=15.63$ ($\delta c=41.5$), $s=32.69$ ($\delta c=86.6$)

FIG. 5. Comparison of the states of distorted grid pattern at nearly same degree of die closure where blanks listed in Table 1 have been shaped by fundamental tools lubricated by vaseline. $h_0b_0=1.056$, $H/B=0.3$, $A/B=0.6$, $W/B=1.2$.

Therefore, these stages may be referred to as the "cutting stage".

After this stage, as the ratio of the flash w/t increases, the deformation comes up to a stage where the material in the joining region can not move without plastic deformation. In this process material in the rim rises as if it were a rigid body floating on the plastic mass. This deformation mode appears when free surface of the rim does not reach the depth end and the ratio w/t is

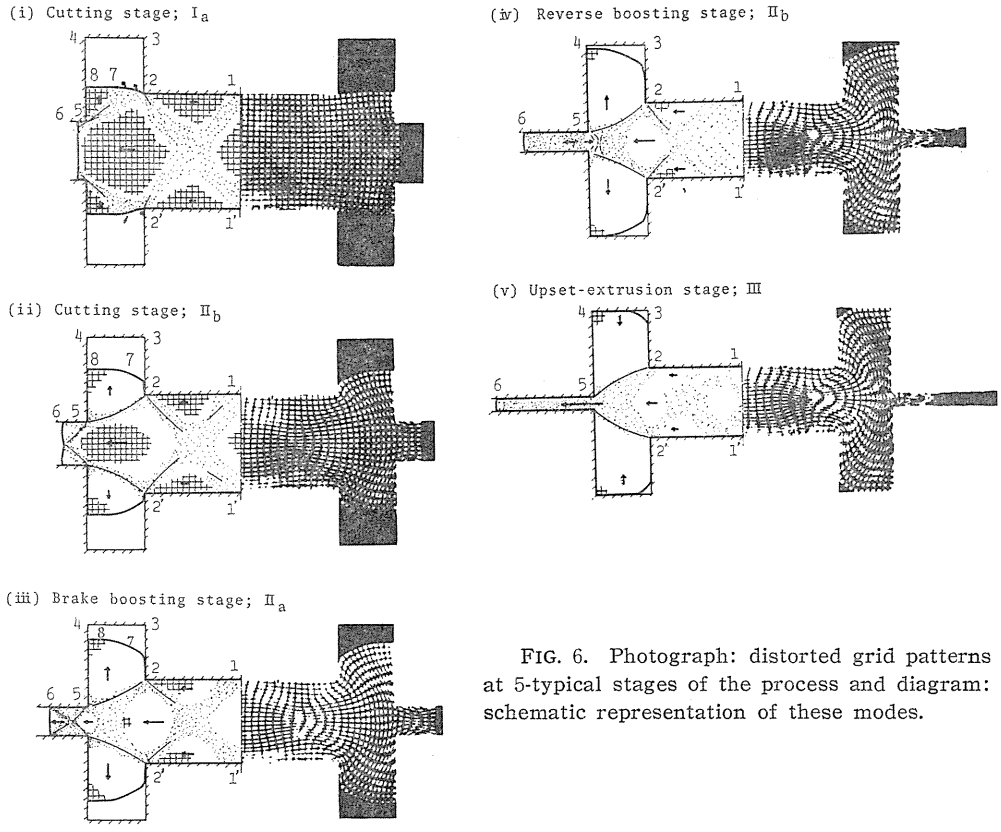

FIG. 6. Photograph: distorted grid patterns at 5-typical stages of the process and diagram: schematic representation of these modes.

kept within a limited value. In this stage the filling velocity of the rims seems to be enhanced by the brake action of the flash, so it may be referred to as the "brake-boosting stage".

When the thickness of the flash t becomes less and its length w larger so that the ratio w/t exceeds a critical value which is defined by friction of the flash-land, a neutral line or shedding region of material flow takes place near the entrance of the flash and a part of the material begins to flow reversely into the joining region. As a result of this reverse flow, the filling-in action of the rims is so accelerated that this stage may be referred to as the "reverse-boosting stage".

After the rim tip touches the depth end of the die, corners of the rim cavity are filled-up gradually with the adjacent material. In accordance with this filling-up of the cavity corners the reverse flow from the flash becomes depressed and finally, all of the surplus material comes to be extruded out through the flash-land to the gutter by the squeezing action which takes place in the web and the joining regions. See Fig. 6 (iv) and (v). This final stage may be called "upset-extrusion stage".

Summing up the above, in a compound flow which occurs during the die forging process there can be noticed four distinguished types of deformation modes *i.e.* "cutting", "brake-boosting", "reverse-boosting" and "upset-extrusion".

These deformation modes are idetified by the symbols I, II_a, II_b and III respectively in Fig. 6. Hereafter, the critical moments in the process when the deformation mode chages will be referred to as follows:

The critical point C; deformation mode changes from I to II_a, the critical point R; deformation mode changes from II_a to II_b, the critical point F; deformation mode changes from II_b to III.

And the supposed ultimate stage when flash height $2t$ becomes zero will be defined by U.

By experiment where the tools of the fundamental form are used, the authors will explain below how the occurrence of these critical stages is affected by a change in the volume of surplus material.

4.2. Horizontal displacement of material along the parting line

Assuming that the die engraving is symmetric about its parting line, characteristics of the material flow will be clarified by tracing the displacement of material on the symmetric plane or the parting plane. On the sectional plane of the blanks shown in Fig. 7 (above), numbers from 1 to 27 are given to the constant-spaced grid points on the parting-line, being counted from center to out side. Curves in Fig. 7 show plots of the horizontal displacement u_X of each point in relation to the die stroke s. The broken lines and chain lines correspond to the points which occupy central and outside regions respectively. They seem to increase monotonuously with the die stroke. The intermediate points from 14 to 27, represented by full lines, seem to make the most extensive displacement until a certain earlier point of the process. See point C in Fig. 7. This means that until this point, the material between these numbers has moved translatively as a rigid body. However, this single solid line begins to part off after C. This means that plastic deformation occurs in the material belonging to this joining region. According to the bifurcation of curves at C the deformation mode changes from I to II_a at this point.

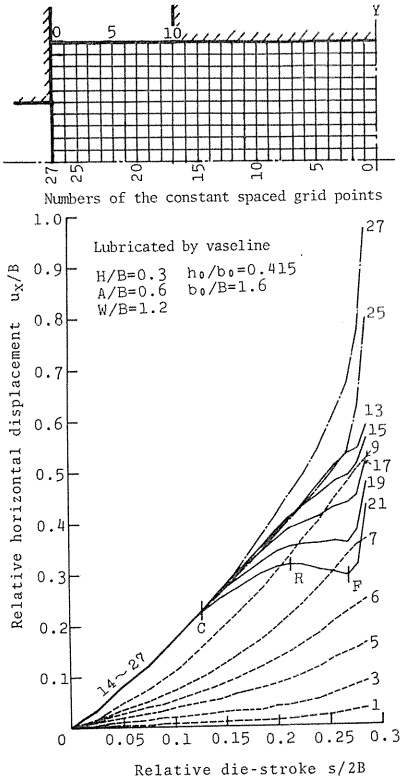

FIG. 7. Diagram of the horizontal displacement of elements on the parting line.

The maximum point R of curve 21 shows that an inverse flow from the flash to the joining region starts. And so, this maximum corresponds to nothing but the critical point R. Since the slope of all these curves represents horizontal velocity, when a curve changes its slope abruptly, a sudden change in the direction of flow should be thought to have occurred somewhere. As will be seen in the curve 21 at point F the process comes under this change,

so it should be thought that the belonging material starts an intense outward flow at this point. The point F is thus called the critical point for upset-extrusion.

As stated above, it has been found that the critical points C, R and F can be defined clearly by tracing the horizontal displacement of particular elements on the parting line. Therefore, in the following, examinations of the material flow will be done based on the displacement curve like those represented by solid lines in Fig. 7.

4.3. *Effect of surplus material and the height-width ratio of blank on occurrence of the change of modes*

The blanks listed in group II of Table 1 have a common width of $2b_0=80$ mm, and have different heights or volumes. The horizontal displacement curves for these blanks are shown in Fig. 8. Though the critical points seem to come earlier with a decrease in the surplus material, this will not be the case when the filling-up point F disappears because of lack of the blank material. On the other hand, if critical points R and C disappear before filling-up because of much surplus material, the boosting effect of the flash will not be available, and this leads to an excess of forming energy because of an increase in the rate of process after the point F.

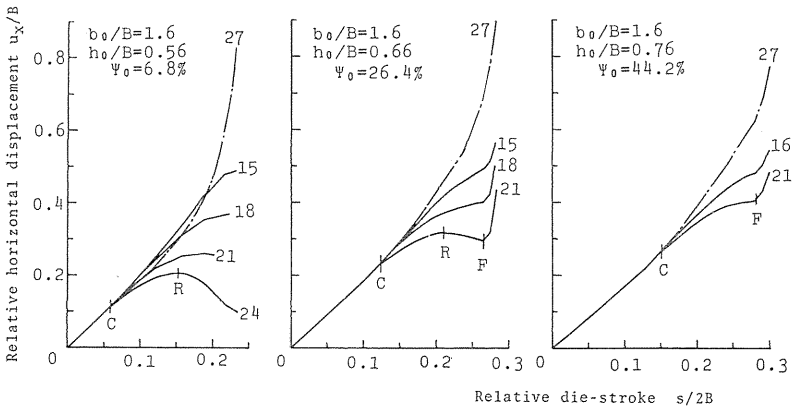

FIG. 8. Horizontal displacement curves (Effect of surplus material. $A/B=0.6$, $H/B=0.3$, $W/B=1.2$. Lubricated by vaseline).

Fig. 9 shows a diagram in which critical points for the case mentioned above are plotted. If a defined percentage of surplus material is imagined in Fig. 9, it will be possible to draw a parallel line to the abscissa, and by doing so, the moment at which the deformation mode changes can be predicted knowing the intersection of this line and each critical line. The section length of this line between F- and U-lines corresponds to the flash height taken when the die cavity has just filled up. The minimum allowable surplus material can be estimated as about 3% by reading the ordinate of the point at which the curve F and the line U intersect.

Blanks listed in Table 1-group I have the same volume but different shape-ratios. When they are deformed by the fundamental tools, the simple upsetting stage increases with an increase of the blank height. This circumstance is seen

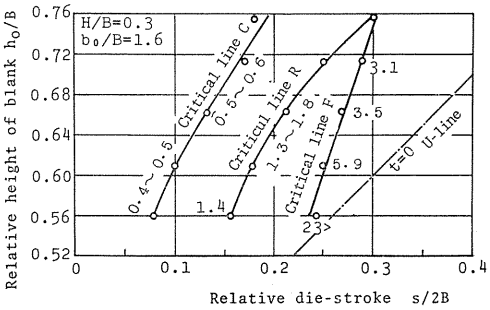

FIG. 9. Diagram of the critical points (For the dies of the fundamental form. Lubricated by vaseline). Attendant figures of the plotted curves show $w/2t$ assumed at the critical points.

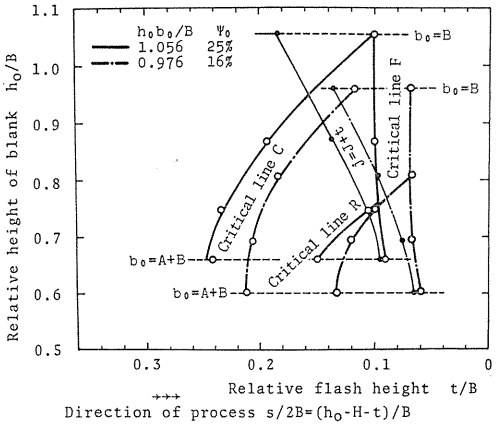

FIG. 10. Diagram of the critical points (Effect of the height-width ratio of blank. Lubricated by vaseline).

in (b), (c) and (d) of Fig. 5. Therefore, in a tall blank the critical point comes later and thus a reverse flow from the flash to the joining region will become difficult to occur because the rim tip can touch the depth end of the die before development of the flash. The diagram of critical points for this case is shown in Fig. 10. The abscissa in Fig. 10 is dementionless flash height t/B instead of $s/2B$ in Fig. 9. The curve $j=J+t$ may be considered to be a kind of critical line which means that, on this line, the tip of the rim just touches the depth end surface of the die. If the process is observed on the basis of t/B, inclined tendencies of the critical lines C and R show much differences according to the shape ratio of the blank even when the volume is constant. In a very tall blank, the critical point F comes slightly earlier than in a dwarf one.

4.4. *Effect of the dimensional parameters of the die on occurrence of the critical points*

It might be supposed that the die dimensions H, J and W among shape parameters of the die would certainly affect the material flow. Since percentage of the surplus material ψ_0 differs according as alteration of H or J, it would be necessary to take this change into account in examination of the effect of these parameters on the critical point. H is the depth of a web-face which should be nearly equal to the final web thickness. Therefore, H appears to control the stroke duration of the cutting stage and thus to affect the degree of deformation. To ascertain this, blanks listed in Table 1-II were shaped by the tools having $H/B=0.1$, and as a result, a critical point diagram has been obtained as shown in Fig. 11. Comparing this result with Fig. 9, it will be realized that critical points come later when H/B is small. Thus, in this case, more material flows out into flash for the same amount of the die closure.

The width of the flash-land appears to have an effect of primary importance on the material flow in the joining region. So, in Figs. 9 and 11, the values of the width-height ratio of the flash w/t which are assumed to take place at the critical points have been indicated by figures added along the plotted curves. It

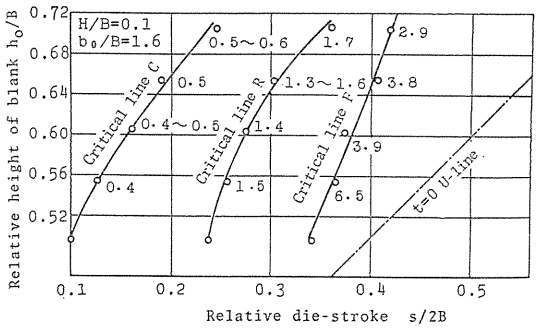

FIG. 11. Diagram of the critical points (For the die having $H/B=0.1$. Lubricated by vaseline). Attendant figures of the plotted curves show $w/2t$ assumed at the critical points.

seems that when the flash-land width W is sufficiently large, for the deformation mode to change during a process w/t must exist within the following limited ranges:

$w/t=0.8\sim1.3$ for the critical point C,
$w/t=2.8\sim3.2$ for the critical point R.

For occurrence of the critical points, w/t can be said to be an influential factor whenever in a process the mode of flow changes. Therefore, if W is defined within certain limits, the occurrence of critical points must be adjusted. To ascertain this, the standard blanks ($b_0=A+B$, $h_0/b_0=0.451$) have been shaped by the dies whose W is altered as shown in the above of Table 1.

Fig. 12 shows the horizontal displacement diagram in this experiment. It may be realized that the horizontal velocity of material on the parting line cannot tend downward during a process in the case of the smallest W. This result tells that the changes of mode at C and R have been brought about by slip resitance of the flash-land. It follows from this that if W is so small that, during a process, the value w/t cannot come under the range of values mentioned above, an enhancement of die-filling by the flash land resistance will not be available.

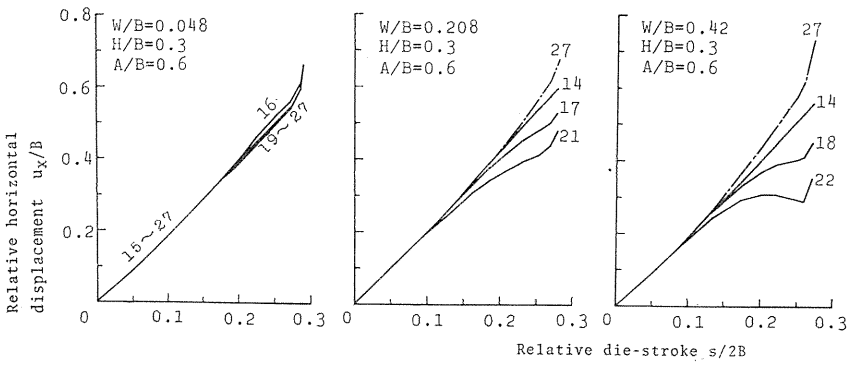

FIG. 12. Horizontal displacement curves (Effect of alteration of flash land width. Lubricated by vaseline. $h_0/b_0=0.415$, $b_0/B=1.6$).

4.5. *Filling-up of the rim (Das Steigen)*

Material of the grid spaces numbered from 17 to 27 is situated below the rim cavity at first. See Fig. 5 (a) or Fig. 7. In the process, the free surface

toward the cavity being numbered 0 to 10 in Fig. 7 (above) rises for the most part keeping itself free until it touches the depth end of the die as will be seen in Fig. 13 (a) and (b).

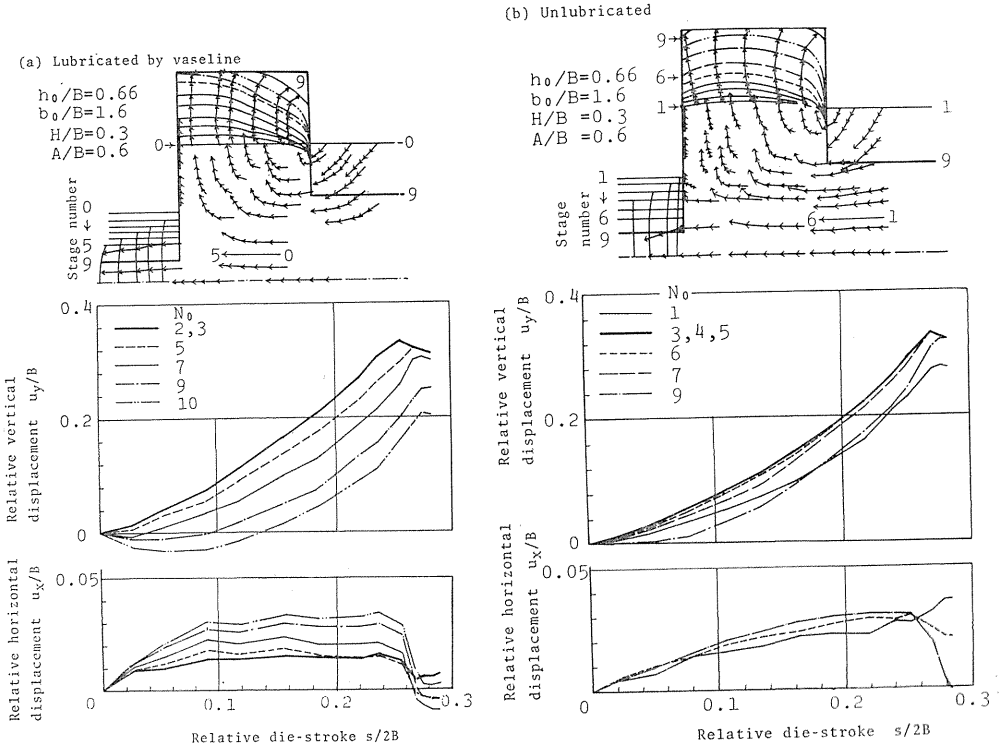

FIG. 13. Filling of the rim.

In Fig. 13 (above), degrees of die closure are specified by numbers from 0 to 9 and the corresponding outlines of the free surface are shown by repeated lines. Small arrows in the figure indicate the corresponding positions of the material points at these stages (*i.e.* (a) 0→5 and (b) 1→6). The difference between (a) and (b) comes from that of lubrication conditions.

Diagrams in Fig. 13 (below) show the vertical and horizontal displacements of the points on the free surface of the rim (As stated, numbers 0 to 10 are designated from the outermost grid point. See Fig. 7 (above)). These curves, being almost parallel with each other, show that shape of the free surface does not change markedly during a process. It follows from this that the deformation of the free surface is said to be almost settles after a certain initial stage.

The differences which are observable between (a) and (b) can be explained by slip-line field applicable to the cutting stage which was referred to elsewhere. See reference 43). For other details see the figure.

4.6. Sequence diagram of material flow in the die

In the material flow treated so far, the dimensions A and B have been kept constant but other parameters varied so as to clarify the conditions when the

deformation mode changes. In the diagrams of critical points as shown in Figs. 8, 9 and 10, however, an understand of the development of deformations in various portions of die-passages at the same time is said to be still difficult. For the sake of the simultanious knowledge of the change of various parameters during the process, the sequence diagrams for a forging process as shown in Figs. 14, 15 and 16 are proposed. In these figures, the parameters adopted are width-height ratio of the flash w/t, sectional area of the flash $F_f/4B^2=wt/B^2$ or $(Wt+f)/B^2$, height-width ratio of the rim j/A and the specific web thickness h/B.

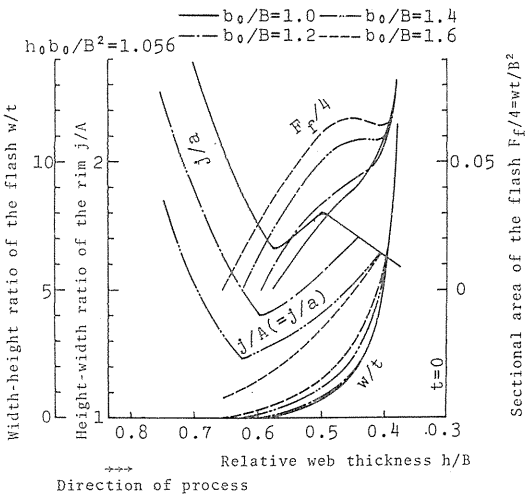

FIG. 14. Sequence diagram of material flow (Lubricated by vaseline. Constant volume of blank. Alteration of width-height ratio of blank. Fundamental tools; $A/B=0.6$, $H/B=0.3$, $W/B=1.2$).

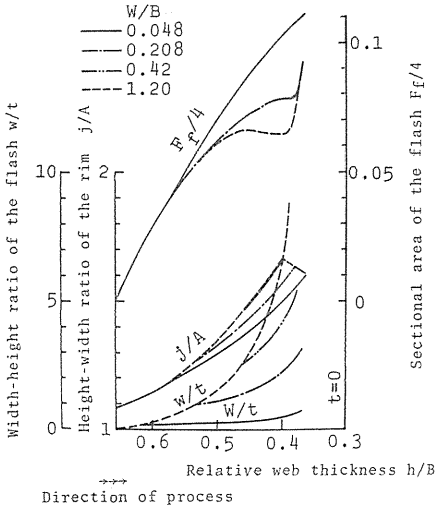

FIG. 15. Sequence diagram of material flow (Lubricated by vaseline. Standard blank. Alteration of flash land. $h_0/B=0.66$, $b_0/B=1.6$, $H/B=0.3$, $A/B=0.6$). In the curves $F_f/4$ and j/A, double dots-dash-lines nearly lie on the broken lines.

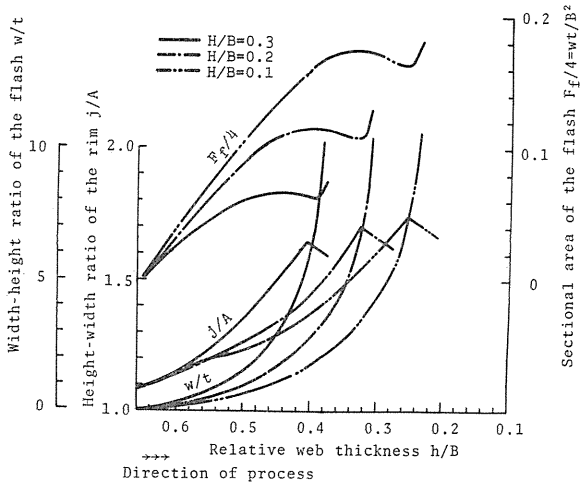

FIG. 16. Sequence diagram of material flow (Lubricated by vaseline. Standard blank. Alteration of sunken depth of the web. $A/B=0.6$, $W/B=1.2$, $J/B=0.9$, $h_0b_0/B^2=1.056$, $b_0/B=1.6$.).

Fig. 14 shows a sequence diagram in which blanks listed in Table 1-I are shaped by the tools of the fundamental form. The abscissa represents h/B instead of die stroke for the convenience of comparison of various blank heights. In this figure, it should be noted that the critical point C comes at a stage when the value w/t reaches about 1 and the critical point R comes at w/t of about 3. The curve $F_f/4B^2$ shows a maximum or an inflection at the critical point R. The curve j/a shows somewhat severe undulation due to characteristics of this value. At its minimum the material is supposed to reach the entrance of the flash land when the variable 'a' becomes just equal to the rim width A. Whereas, at its maximum, the material of the rim tip reaches the depth end of the die. Since the critical point F should come a little after this maximum, the tendency of the curve j/A or j/a may be said to give a key to finding the point F.

Fig. 15 shows a sequence diagram where standard blanks are shaped by the dies whose flash land width W is altered. As will be supposed, the critical point C comes at the time when the value of w/t reaches about 1.

It seemed convenient that in order to define the point R, one should have recourse to the maximum point of $F_f/4B^2=wt/B^2$. For a value of $W/B=0.0048$ critical conditions C and R could not happen.

The sequence diagram for various dies whose step height H's are different is shown in Fig. 16. Critical points C and R, and accordingly, the tendencies of parameters w/t, $F_f/4B^2$ and j/A are strongly affected by the change of step height H. Therefore, it might be stated that step height H is one of the most important among the parameters which control the die-filling.

In any diagram, $F_f/4B^2$ should increase rapidly after the critical point F.

5. Geometry of deformation in axi-symmetric condition

There are many axi-symmetric components such as gear wheels, and other circular forgings as well as two-dimensional forgings such as connecting rods, levers and support beams, all of which are composed of rib and web portions. In an axi-symmetric forging, the relative volume of the rim portion to the total volume will be different according to the radial position of the rim. This is not the case in plane strain forging. The radial displacement of a material element always accompanies circumferential plastic strain which makes the material difficult to flow radially in the joining region. Therefore, in the case of axi-symmetric rib and boss formation, it is very important to know the specialities of the radial flow of this kind.

In this section, the plasticine experiment on the axi-symmetric condition will be referred to. The differences between the axial symmetry and the plane strain in the filling-in phenomena will be visualized by the diagrams of the horizontal displacement, the critical points and the sequence.

5.1. Horizontal displacement of material and the deformation modes

The horizontal displacement on the parting line in axi-symmetric models was measured by step-by-step photographing. One example of the displacement diagrams where the blank with 34.9% surplus material is shaped by the tools of the fundamental form is shown in Fig. 17. Curves numbered from 1 to 34 correspond to the displacement during the process for the constant-spaced concentric

circles in the initial state. See Fig. 3 (b). The material of the space numbered from 22 to 34 is situated below the rim-cavity at first. The slopes of all curves correspond to the horizontal velocity of the referring element.

Although each slope of the curves is about 1/2 of that in plane strain, the tendency of the curves will be found to be similar to that in plane strain. Therefore, the critical points R and F can be defined clearly by means of tracing the horizontal displacement curve of 26 in Fig. 17. But the critical point C cannot be found until this diagram is compared with the diagram in Fig. 18 where the same blank is shaped by the die whose flash land width W is altered to the smallest value in Table 2. Because radial displacement velocity in the joining region always decreases with an increase of the radial position irrespective of the frictional resistance of the flash land or the boosting action.

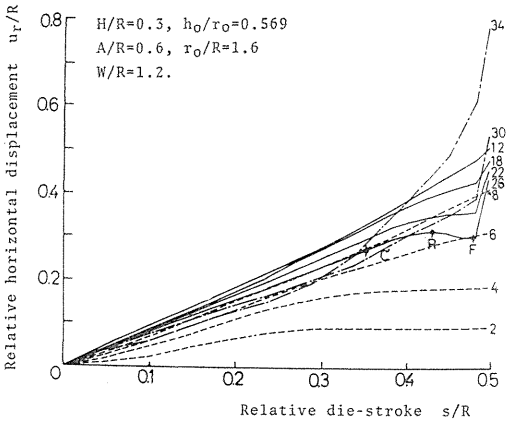

FIG. 17. Relation between die-stroke and horizontal displacement of the elements which lie on the parting plane or r-axis in Fig. 3 (Axial symmetry; centrifugal flow. Lubricated by vaseline).

The critical points C, R and F are thus, estimated and indicated in Fig. 17. It may be stated from this that the sequence of the same typified modes of de-

TABLE 2. Geometrical conditions of the die and the blank for axial symmetry

Shape parameters in the die

	Centrifugal flow		Centripetal flow	
	Fundamental	Altered	Fundamental	Altered
Width ratio of the rim and the web A/R	0.6	0.48, 0.38 0.28, 0.18	0.6	0.167, 0.75
Height-width ratio of the web H/R	0.3	0.1, 0.2	0.3	0.1, 0.2
Height-width ratio of the rim J/A	1.5		1.5	
Radial position of the entrance of flash R_0	50.2 mm		35 mm	
Flash land width W	42.4 mm	1.0 mm, 10 mm	35 mm	1 mm

Shape parameters of blank

	Centrifugal flow			Centripetal flow		
	φ_0	h_0/b_0	h_0 mm	ψ_0	h_0/b_0	h_0 mm
Standard	34.9	0.569	28.5	38.3	0.413	14.46
Altered	6.0 18.5 48.0 62.8	0.447 0.500 0.624 0.686	22.4 25.1 31.3 34.4	16.1 26.6 59.5	0.347 0.378 0.477	12.42 13.24 16.68

formation as we have observed in the plane strain condition also occurs in the axi-symmetric condition.

5.2. Interrelation between occurrence of the critical points and relating geometry

Blanks having a common diameter $2r_0=2(R+A)$ but different heights were shaped by the fundamental tools to find the critical points C, R and F in axi-symmetric condition. The result is shown in Fig. 19. In the figure, solid lines indicate the axial symmetry and chain lines indicate the plane strain. Supplemental scales of the percentage of surplus material ϕ_0 are also added to the ordinate. In comparison of Fig. 17 and 18, by noticing the difference between the curve 26 which shows the utmost fluctuations in Fig. 17 and the corresponding curve 26 in Fig. 18, probable point of C could be determined. In the critical points diagram of Fig. 19, it will be easy to see that when the percentage of surplus material are the same in plane strain and in axial symmetry, the deformation modes during a process will be sequenced in a similar manner. In both cases the values w/t, indicated by the attendant figures of the curves at the critical points C and R may exist within the limited ranges corresponding to the variation of h/B or h/R if the ratio A/B or A/R is fixed. Since the critical points C, R and F appear at relatively latter stage in axi-symmetric condition, the cutting mode of deformation will take precedence in a process.

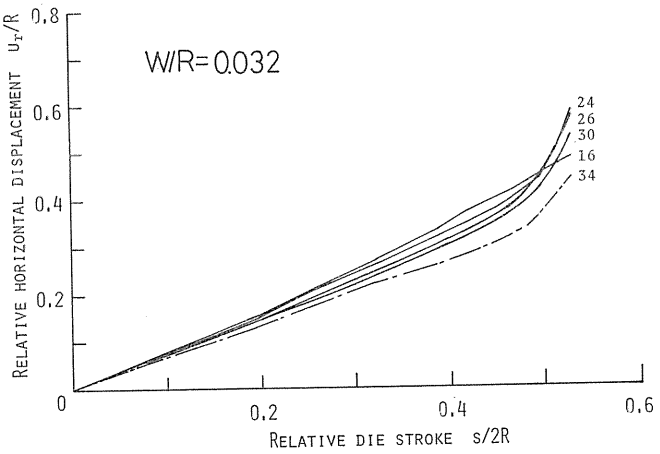

FIG. 18. Diagram of the horizontal displacement of elements on the parting line.

In any case, it was proved that the sequence of the deformation modes during a process; cutting, brake-boosting and reverse boosting, could be affected by the ratio of flash land width to height. In order to ascertain the dependence of the critical conditions C and R on an alteration of the deformation geometry in the die, blanks listed in Tables 1 and 2 are shaped by the die whose dimensions H and A are shown in the same tables. The relations between the values w/t and h/A at C and R are shown in Fig. 20. As the abscissa h/A represnts the geometry of the joining region, the decreasing sense of the value h/A means the direction of the process for a constant A.

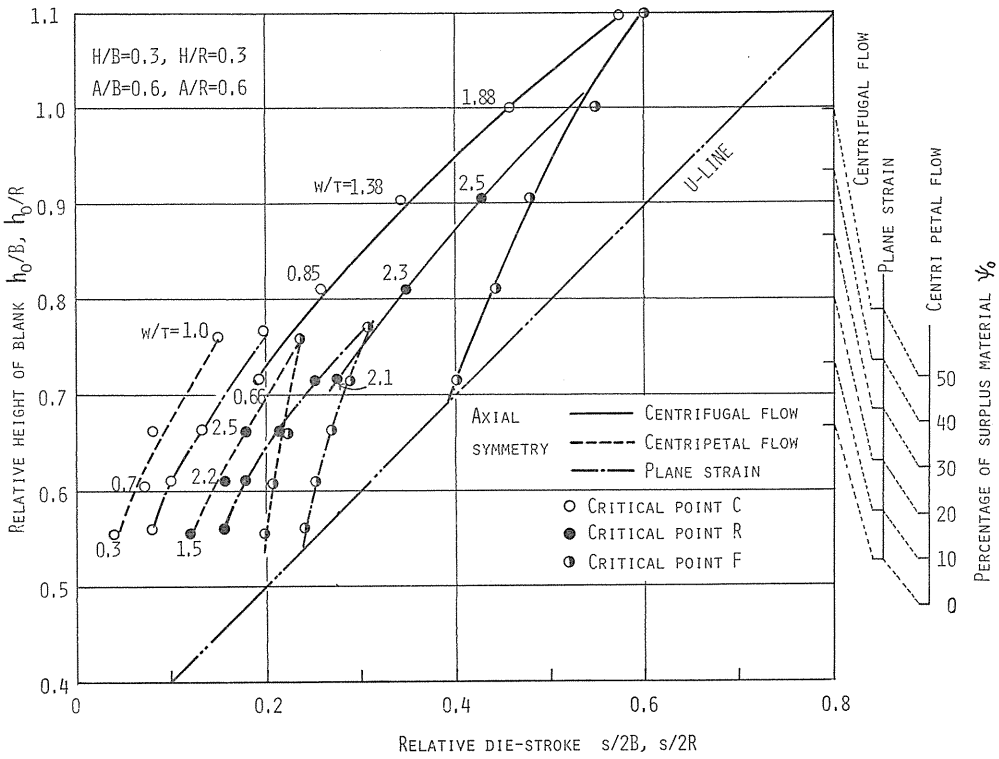

FIG. 19. Effect of the excess material of blank on the occurrence of critical stages when deformation modes change, in relation to the ratio of the flash height and width at those stages (Lubricated by vaseline).

On this coordinate plane, two straight lines C and R can be drawn approximately for both plane strain and axi-symmetric conditions as to pass the plotted points C and R, respectively. These lines, therefore, divide the w/t-h/A plane into three regions; cutting, brake-boosting and reverse-boosting. By plotting the development of w/t with decreasing h/A in this plane, the curve shows the sequence of deformation modes by the intersection as their changing points.

It will be easy to find that in axi-symmetric flow the values at these critical points may be smaller than that of plane strain for any geometry of the joining region h/A.

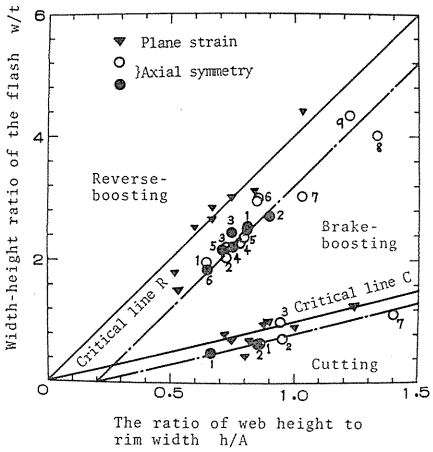

FIG. 20. Interrelation between the ratio of flash width to height and the ratio of web height to rim width at the critical points.

5.3. Filling-in rate at various portions of the axi-symmetric model-die

In the foregoing, it has been found that section geometries w/t and h/A

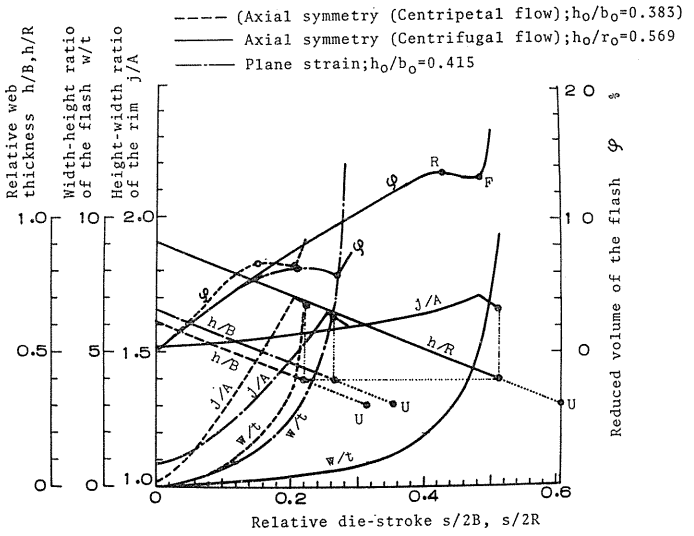

FIG. 21. Sequence diagrams of dimensionless factors which typify the degree of die-filling in the main portion of the die-impression (Tools of the fundamental form).

affect the sequence of deformation modes. In order to understand specialities of die-filling under axi-symmetric conditions, it will be necessary to compare the sequence diagrams of axial symmetry with that of plane strain.

In the sequence diagrams shown in Fig. 21, it is expected that the section geometries of the material in both cases take simillar figures at the critical point F. In axi-symmetric condition, it will be noticed that w/t, solid lines in Fig. 21, increases more slowly than in plane strain. And so the critical points C and R in this condition happen to come later. Therefore, one cannot expect to perform a process in the benefit of the boosting stage. Since the vertical movement of the rim tip Δj is little in axi-symmetric condition, the rim is said to be shaped mainly as a result of indentation of the web faces. So, a more stroke is necessary to fill up the rim cavity. Relative volume of the flash φ at the critical point F comes up to twice as much as that in plane strain.

If the flash height $2t$ and its width w are measured, mean total height of the rim $\bar{j}/A$ can be easily calculated by

$$\bar{j}/A = [r_0^2 h_0 - R^2 h - tw\{w + 2(R + A)\}]/\{A^2(A + 2R)\}, \tag{5.1}$$

and mean rise of the rim tip $\Delta\bar{j}/A$ is given by $\bar{j}/A - h_0/A$.

Fig. 22 shows the variation in $\Delta\bar{j}/A$ with $s/2R$. It becomes evident from Fig. 22 that total height of the rim for small H/h_0 and A/R even decreases during a process. In the cutting stage of axial symmetry where the material in the joining region flows centrifugally, the axial strain rate $\Delta\varepsilon_z/\Delta s$ in the joining region is less than zero and its mean value decreases with a decrease of A/R as shown in Fig. 23. In addition, the material originally situated in the joining region plays more important part for the filling of the rim than the material which is newly extruded into the joining region from the web portion.

Consequentry, the increase of total height of the rim is not always attained unless the forging parameters H, A, h_0 were determined in due regard to the states mentioned above. Since the mechanism of the rim formation in axi-symmetric condition is rather similar to that of piercing, it will be advantageous to pass through the initial free upsetting stage by utilizing the blank whose diameter is less than $2(R+A)$.

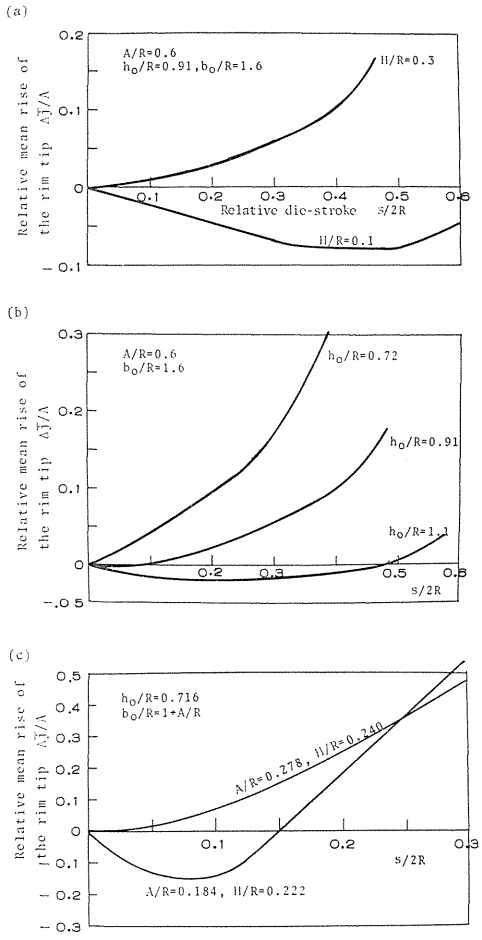

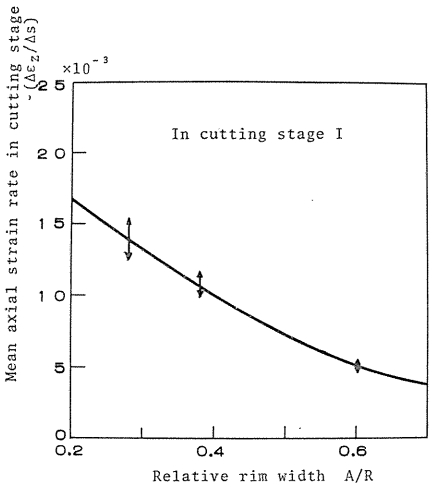

FIG. 23. Relation between relative rim width and mean axial strain rate in the joining region. Lubricated by vaseline.

FIG. 22. Effect of the forging parameters on the rising height of the rim (Axial symmetry; centrifugal flow. Lubricated by vaseline).

6. Mechanisms of the rim and boss formation

As stated before, five typical modes of deformation including a free upsetting stage along with the former four stages were observed in the regions joining the rim and the web. In the boosting-stages of the deformation, filling-in velocity of the rim could be enhanced. It was found also that a difference in the filling-in velocity existed between the plane strain and axial symmetry.

In this section, in order to arrive at a quantitive understanding relating to the filling phenomena, the upper bound technique is applied to the possible mode likely to occur in the joining region. For this kind of compound flow, it may

be necessary to consider the states of deformation as shown in Fig. 24. In the figure, the vertical passage may be called the rim or the boss. Material in the horizontal passage which may be identified by the name, web or flange, will be extruded to flow into the rim and into the other horizontal passage which forms the flash-part. In axi-symmetric conditons the material beneath the web flows centrifugally to fill the rim cavity, while the material beneath the flange flows centripetally to fill the boss cavity.

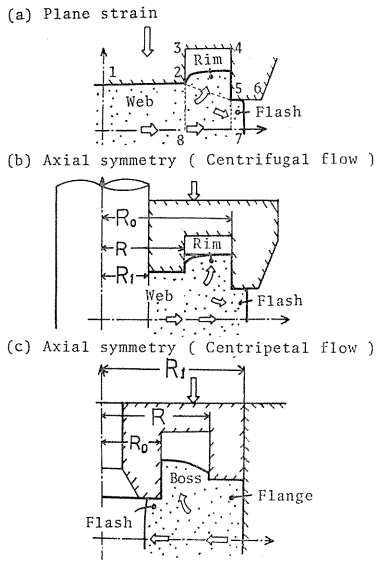

FIG. 24. Schematic diagrams of the three deformation types.

If the ratio R/A becomes very large keeping geometry of the rim and flash sections similar, the deformation in the passages as shown in Fig. 24 (b) and (c) will become equivalent to the case (a). Consequetnly, in axi-symmstric flow the ratio R/A or A/R must have an significant effect on the filling-in phenomena. In the joining region of Fig. 24 (a), the material is supposed to move across the section 25 and 57 at the velocity v_J and v_F, respectively. And the extruding velocity from web across the section 28 is designated by v_A and the half of the closing velocity of the dies by v_S. Other parameters or dimensions are shown in the figure.

Assuming that the material is incompressible, the following relations between the variables can be written

$$v_J = (h/A)\{1-(1\pm A/R)(1-H/h)\alpha\}v_A/(1\pm A/2R), \tag{6.1}$$

$$v_A/v_S = (B/2h)(1+R_1/R), \tag{6.2}$$

where $\alpha = v_F/v_A$ and the plus and the minus signs of the complex symbol $\pm$ correspond to the centrifugal flow model and the centripetal flow model respectively. See Fig. 24 (b) and (c). Since A/R may be taken as zero for the plane strain condition, the above equations in plane strain can be reduced to

$$v_J = (h/A)\{1-H/h)\alpha\}v_A = (B/A)\{1-(1-H/h)\alpha\}v_S \tag{6.3}$$

$$v_A/v_S = B/h \tag{6.4}$$

It follows from the above equations that filling-in velocity of the rim is mainly affected by the geometry represented by B/A, A/R, H/h and by the velocity ratio $\alpha = v_F/v_A$ whose value is closely concerned with the deformation modes. In experiment, it was found that α could be determined from the rate of the flash volume per unit penetration $\Delta V_f/\Delta h$. That is,

$$\begin{aligned}\alpha &= (\Delta V_f/\Delta h)(v_S/v_A)/\{2\pi R_0(h-H)\}\\ &= \{\Delta\varphi/\Delta(h/A)\}(v_S/v_A)\{h_0 b_0(r_0+R_1)\}/(2tR_0)\end{aligned} \tag{6.5}$$

where $b_0 = |r_0 - R_1|$.

In the following, the sequence of deformation modes and the relating load characteristic which may be changed by the parameters mentioned above will be discussed.

6.1. Velocity fields of the typified deformation modes

Various methods of analyses which can explain a finite deformation were suggested so far. In the present problem, the deformation is so complex that the analysis applicable is desired to be simple. The Kudo's upper bound method seems to be suitable under these circumstances.

As stated before, five stages of deformation typified and the belonging four critical points will be denoted by symbols listed in the table below.

Stage	Symbol	Critical point
Free upsetting	O_s	O_s
Cutting a	$\mathrm{I_a}$	
Cutting b	$\mathrm{I_b}$	C
Brake-boosting	$\mathrm{II_a}$	R
Reverse-boosting	$\mathrm{II_b}$	F
Upset-extrusion	III	

According to the observation of the flow patterns in plane strain condition, it seemed that the typical velocity fields might be represented by the numbered blocks shown in Fig. 25. These velocity fields in plane strain condition are composed of rigid blocks of material separated by lines of discontinuity as shown in the figure. On the other hand, in axi-symmetric conditions some plastic work must be dissipated even in a region surrounded by discontinuity lines whenever a horizontal movement of the blocks occurs. Assuming that the axial velocity component v varies linealy with the z-coordinate, the velocity components beneath the web in any deformation modes may be defined by

$$\left.\begin{array}{l} u=0 \\ v=-1 \end{array}\right\} \text{ in zone 1, } \quad \left.\begin{array}{l} u=R/2h \\ v=-(R/2h)(z/r) \end{array}\right\} \text{ in zone 2}$$

in accordance with a unit downward velocity of the upper die v_s of -1.

In the rim and the joining region, the velocity components for free upsetting stage are

$$\left.\begin{array}{l} u=\{2R\eta_3 v_A-a(2R+a)v_J\}/(2r\eta_3) \\ v=-v_J\cdot z/\eta_3, (\eta_3=\text{constant.}) \end{array}\right\} \text{ in zone 3,}$$

For cutting stage, they are

$$\left\{\begin{array}{l} u=\{2hRv_A-(r^2-R^2)v_J\}/(2r\eta_3) \\ v=\{v_J-(H/A)u\}z/\eta_3 \\ \eta_3=h-(H/A)(r-R) \end{array}\right\} \text{ in zone 3, } \quad \left.\begin{array}{l} u=0 \\ v=v_J \end{array}\right\} \text{ in zone 4,}$$

while for boosting stage, they are

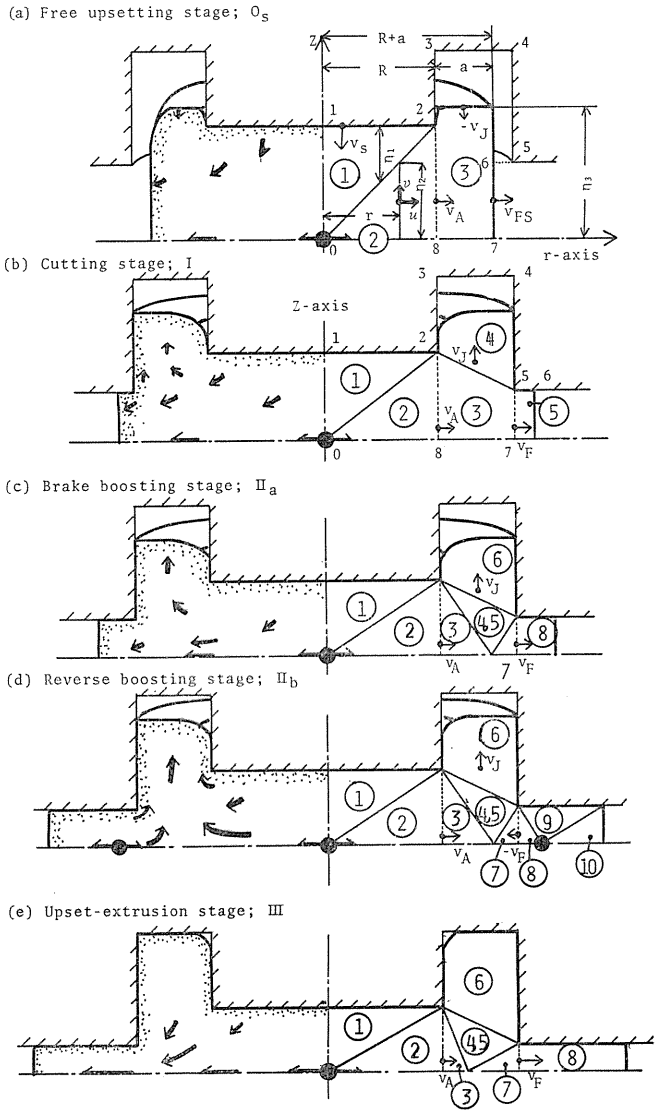

FIG. 25. Five typical types of velocity field; Axial symmetry. Centrifugal flow model.

$$\left.\begin{cases} u = v_{12}(R_4^2 - r^2)/(2r\eta_3) \\ v = \{v_{12} - u\cdot h/(R_4 - R)\}z/\eta_3 \\ \eta_3 = h(R_4 - r)/(R_4 - R) \end{cases}\right\} \text{ in zone 3,}$$

$$\left.\begin{cases} u = (v_{12} - v_J)(r^2 - R^2)/(2r\eta_4) \\ v = [v_J - v_{12} + u\cdot\{h/(R_4 - R) - H/A\}](z - \eta_4)/\eta_3 + v_{12} - u\cdot h/(R_4 - R) \\ \eta_4 = 2t(r - R)/A \end{cases}\right\} \text{ in zone 4,}$$

$$\left.\begin{cases} u = (R_0^2 - r^2)(v_J + v_{34})/(2r\eta_5) \\ v = [v_J + v_{34} - u\cdot\{h/(R_4 - R) + H/A\}](z - \eta_7)/\eta_5 \\ \eta_5 = 2h(R_0 - r)/A,\ \eta_7 = t(r - R_4)/(R_0 - R_4) \end{cases}\right\} \text{ in zone 5,}$$

$$\left.\begin{matrix} u = 0 \\ v = v_J \end{matrix}\right\} \text{ in zone 6,} \quad \left.\begin{matrix} u = (r^2 - R_4^2)v_{34}/(2r\eta_7) \\ v = \{v\cdot h/(R_4 - R) - v_{34}\}z/\eta_7 \end{matrix}\right\} \text{ in zone 7,}$$

where $v_{12} = 2Rhv_A/(R_4^2 - R^2)$, $v_{34} = 2R_0tv_F/(R_0^2 - R_4^2)$, $v_J = (2Rhv_A - 2R_0tv_F)/\{A(R_0 + R_1)\}$ and $R_4 = R_0 - At/(h + t)$.

The total energy dissipation rate $\dot{E}$ can be obtained by adding the deformation energy rates of various zones and energy rates due to velocity discontinuities along the boundaries of each deformation zone and the tool material interfaces. The unknown parameters v_{FS} in O_S-stage, v_F in I and II stages and R_4 in III-stage should be determined so that the rate of total energy dissipation in each deformation mode becomes minimum. These conditions are

$$\delta\dot{E}_{O_S}/\delta v_{FS} = 0, \qquad \delta\dot{E}_{\mathrm{I}}/\delta v_F = 0, \qquad \delta\dot{E}_{\mathrm{III}}/\delta R_4 = 0 \tag{6.6}$$

6.1.1. Free-upsetting stage O_S and the shape of the blank

A part of the blank hangs over the joining region by the amount a_0 at the begining. If a_0 is smaller than the rim width A, free-upsetting stage of deformation will continue until the material begins to flow into the flash. Let the web half thickness at the critical moment O_S be designated by h_S. Then, the die-stroke s_0 in the free upsetting stage will be given by

$$\begin{aligned} s_0 &= 2(h_0 - h_S), \\ A - a_0 &= -\int_{h_0}^{h_S}(v_{FS}/v_S)\delta h = -\int_{h_0}^{h_S}\alpha_S(B/h)(1 + R_1/R)\delta h. \end{aligned} \tag{6.7}$$

where the velocity ratio $\alpha_S = v_{FS}/v_A$ is taken instead of $\alpha = v_F/v_A$, and v_{FS} denotes the velocity of the point 7 in Fig. 25. If α_S is nearly constant for $h_0 \geqq h \geqq h_S$ and $\bar{\alpha}_S$ is the mean value of α_S in O_S-stage, h_S/h_0 will be given by

$$h_S/h_0 = \exp[-2(A - a_0)/\{B(1 + R_1/R)\alpha_S\}]. \tag{6.8}$$

Since we take $\alpha_S = 1$ and $R_1/R = 1$ in plane strain, above equations reduce to

$$s_0 = 2(h_0 - h_S) = 2h_0[1 - \exp\{-(A - a_0)/B\}]. \tag{6.9}$$

Hence, the volume of material flowing into the rim cavity during O_S-stage can be given by

$$\begin{aligned} V_{RO}/V_0 &= 4\{b_0(h_0 - h_S) - h_S(A - a_0)\}/(4h_0b_0) \\ &= 1 - \{(A + B)/(a_0 + B)\}\exp\{-(A - a_0)/B\}. \end{aligned} \tag{6.10}$$

In the axi-symmetric condition, on the other hand, α_S must be so determined to minimize the total energy dessipation which is calculated by the assumed velocity field (a). The calculated α_S which depends on h_0 and a_0/R is shown for the condition $h = h_0$ in Fig. 26. The α_S takes the maximum at $a_0/R = h_0/4R$. If a_0/R

is smallar than $h_0/4R$, the web may be upset together with its overhanging portion. The rim can be shaped only when $a_0/R \geqq h_0/4R$ or $a_0/h_0 \geqq 1/4$. So, in order to aim at the die-filling in free upsetting stage, the height of the blanks should be so determined that a_0 is larger than $h_0/4$.

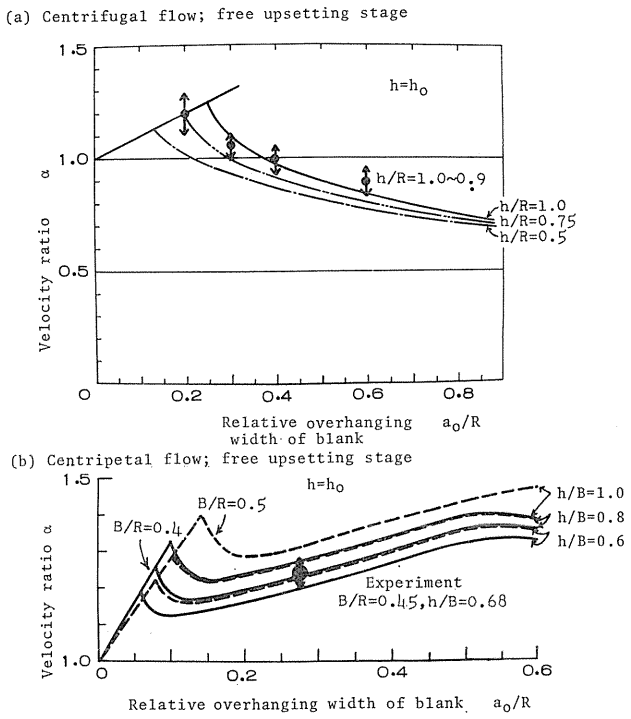

FIG. 26. Relative velocity of out-flowing into the flash
⇕: Experimental value of α or plasticine.
Curves: Calculated value of α for the field in Fig. 25.

Now, the load necessary for free upsetting will be examined. Let the load of the web face and its mean pressure be designated by P_B and p, respectively. P_B will be given by

$$P_B = \pi B(R+R_1)\cdot p = \pi B(R+R_1)\sqrt{3}\cdot k\cdot m \quad \text{for axial symmetry,} \tag{6.11}$$

and

$$P_B = 2Bp = 2B\cdot 2k\cdot m \quad \text{for plane strain.} \tag{6.12}$$

Where k is the shear yield stress of the material and m is the pressure multiplication factor. When the web face is smooth, m is nearly equal to 1 for $a_0 = R_1 = 0$. Hence,

$$P_{BO} = \sqrt{3}\cdot kR^2 \quad \text{or} \quad 4Bk. \tag{6.13}$$

Since this P_{BO} may be regarded as the minimum basic load, hereafter, the working resistance P during a process will be treated by the ratio

$$\tilde{P} = P/P_{BO}. \tag{6.14}$$

6.1.2. Cutting stage I and effect of sunken depth H on the die filling

This deformation stage may be divided into I_a and I_b corresponding to the direction of the discontinuity line in the rim. The deformation in the vicinity of the free surface of the rim is settled by the stage I_b if the friction of the die impression and its draft can be ignored.

On the basis of the velocity fields in the cutting stage, the ratio $\alpha = v_F/v_A$ can be calculated. In plane strain condition α is always equal to 1 in this stage, whereas in axi-symmetric condition, α depends now on the ratio A/R only. Comparison of the experimental α_C and the calculated value of α is shown in the lower curves of Fig. 27. It is observed that the agreement between them is rather good but the experimental α_C in the range of small A/R rather agree with the theoretical α_S which, however, depends on h/B. It may be thought from these results that during the cutting stage α is almost constant irrespective of variations in H/R and h/R.

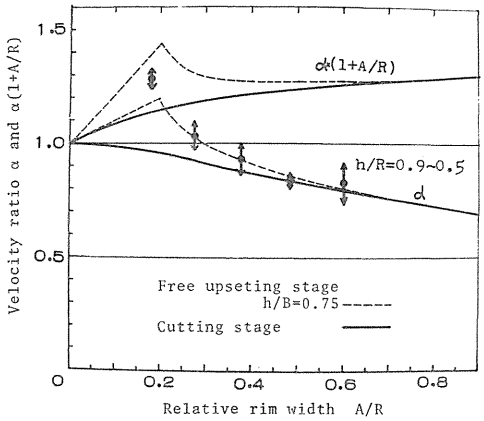

FIG. 27. Relative velocity of out-flowing into the flash in cutting stage.
⇕: Experimental value of α.
Curves: Calculated value of α.

Consequently, if the deformation proceeds from web thickness of $2h_S$ to $2h$ in cutting stage, the volume of material flown into the rim and the flash will be given by

$$\frac{V_f}{V_0} = \alpha_C \cdot G \cdot \frac{B(R+R_1)}{b_0(r_0+R_1)} \tag{6.15}$$

$$\frac{V_R}{V_0} = \frac{V_{RO}-V_f}{V_0} + \frac{(h_S-h)(A+B)(R_0+R_1)}{(r_0+R_1)h_0b_0} \tag{6.16}$$

} for axials ymmetry,

$$V_f/V_0 = G\cdot(B/b_0) \tag{6.17}$$

$$V_R/V_0 = (V_{RO}-V_f)/V_0 + (h_S-h)(A+B)/(h_0b_0) \tag{6.18}$$

} for plane strain,

where $G = (h_S-h)/h_0 - (H/h_0)\ln(h_S/h)$.

In order to increase the total rim height $\bar{j}/A$ through cutting stage, v_J should be greater than zero. This condition is expressed by

$$1/\{1-(H/h)\} > \alpha\{1\pm(A/R)\} \quad \text{from Eq. 6.1,} \tag{6.19}$$

where plus sign applies to centrifugal flow and minus sign to centripetal flow. The sunken depth H of the web can contribute to the filling-in rate in the cutting stage only.

6.1.3. Boosting stage and the critical points R and C.

The velocity v_F or the velocity ratio α tends to decrease with an increase in w/t due to the frictional resistance of the flash land. In this boosting stage,

filling-in velocity of the rim can be accelerated. When the brake action of the flash is intensified more, a part of the material in the flash becomes to flow reversely into the joining region. Therefore, this stage has been divided into II_a and II_b according to the following conditions.

($\alpha=\alpha_C\simeq$constant during a cutting stage I)
$\alpha_C>\alpha>0$: brake-boosting stage II_a
$0\geqq\alpha$: reverse-boosting stage II_b

Fig. 28 shows the sequence of the experimental value α during a process. As will be seen, after point C α changes remarkably with an increase of the boosting action of the flash, it appears very difficult to tell the value α adequately for the various working conditions. A reverse flow from the flash which takes place in the later stage of a process, *i.e.* $t/h\simeq0$, is able to have little effect on the material economy. In addition, it has been seen that the load in II_b increases considerably with an increase of w/t. And so, it will be said to be advantageous that an acceleration of die filling by the boosting must be realized throught the brake-boosting stage. Consequently, relative adjustment of the critical points C and R have an important meaning for improving the die-filling and for the decreasing sake of the forming energy.

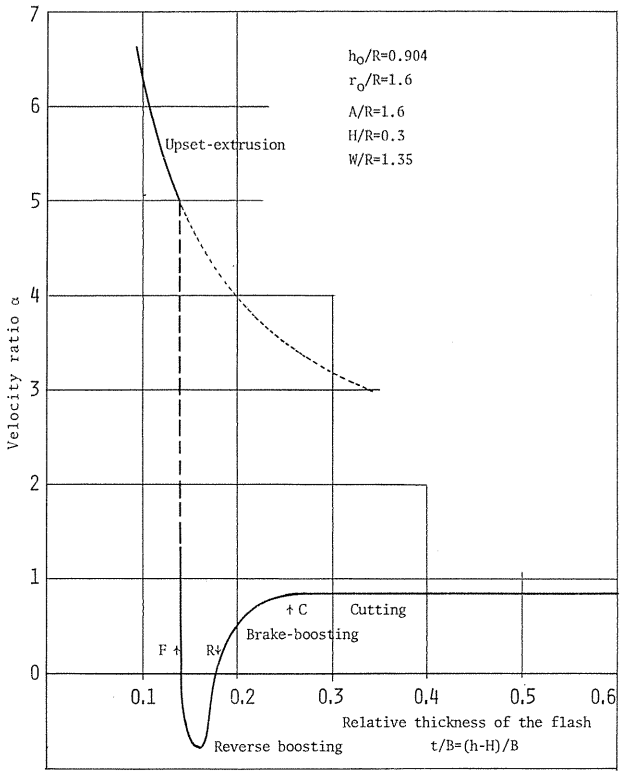

FIG. 28. Interrelation between the relative out-flowing velocity $\alpha=v_F/v_A$ and deformation modes in a process.

If the rate of total energy dissipation of the system is denoted by $\dot{E}$, the critical condition for R may be induced from the condition

$$[\partial \dot{E}/\partial \alpha]_{\alpha=0} = 0. \tag{6.20}$$

In plane strain condition it is expressed by

$$(\tau_F/k)\cdot(w/t) = \{2h + (2j - t - h)(\tau_G/k)\}/A, \tag{6.21}$$

where τ_F: frictional shear stress on the flash land,
τ_G: frictional shear stress on engraving surface.

Whereas, in axi-symmetric condition the above condition of Eq. 6.20 must be given graphically as in Fig. 29 which shows the relation between $(w/t)(\tau_F/k)$ and h/A. The value τ_G is being assumed to be zero in the figures. These critical lines of R, keeping themselves approximately parallel with each other, approach to a line in plane strain of $(w/t)(\tau_F/k) = 2h/A$ with a decrease of A/R. Therefore, critical condition of R may be difined by

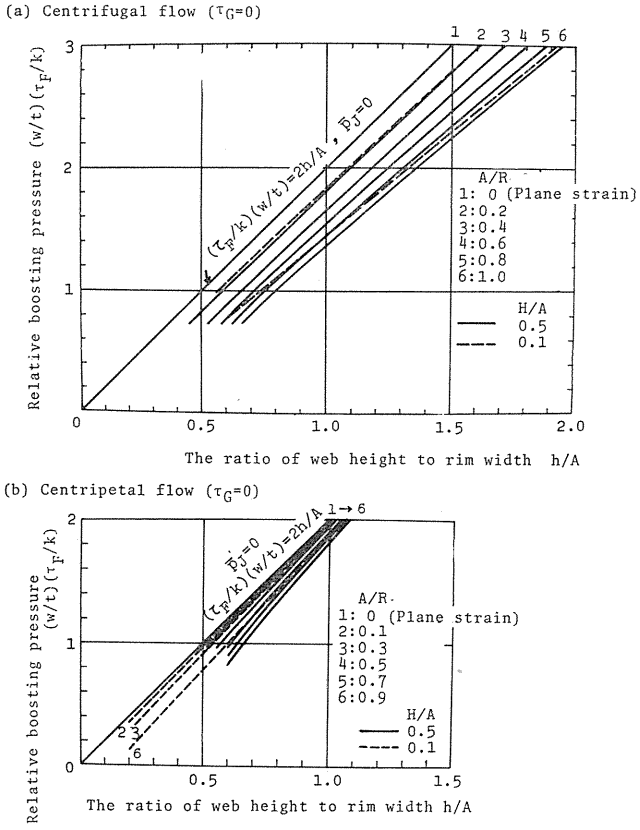

FIG. 29. Interrelation between the mean pressure of the entrance of the flash, $\tau_F w/t$, and the ratio of web height to rim width at the critical points. (Theory)

$$(\tau_F/k)(w/t) = 2(h/A - \Delta) + p_J/k \tag{6.22}$$

where P_J/k is mean extrusion pressure of the rim and Δ is the additive factor of axial symmetry which depends mainly on A/R. The dependence is shown in Fig. 30. Since $(\tau_F/k)(w/t)$ may be regarded as the specific boosting pressure of the flash, in axi-symmetric condition this boosting pressure appears to be reduced by Δ. The agreement between experiment and theory for the critical point of R becomes good if $\tau_F = 0.5k$ is assumed.

On the other hand, based on the experimental results shown in Fig. 20, the critical condition C will be able to be expressed as

$$(\tau_F/k)(w/t) = 0.5(h/A - \Delta) + p_J/k. \tag{6.23}$$

In order to utilize the advantage of the brake boosting action, the flash land width W should be so chosen that the following condition is satisfied before the critical point F.

$$W/t \geq \{2(h/A - \Delta) + p_J/k\}(k/\tau_F) \tag{6.24}$$

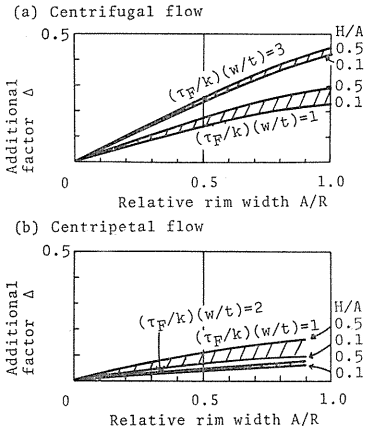

FIG. 30. Additionat factor Δ of axis-symmetric condition for the boosting action of the flash.

6.1.4. *Upset extrusion stage III and the critical point F*

At a certain moment of the cutting or the boosting stage, rim tip will reach at the depth end of the die and after that moment the remaining corner spaces of the cavity tend to reduce rapidly. For this stage I′ the velocity field as shown in Fig. 31 above may be applicable, where the field of the upsetting of asperity proposed by W. Johnson is superposed on the field which holds in the stage of I or II. The mean pressure on the rim tip $\bar{p}_r$ under a plane strain calculated on the assumptions of $\tau_G = 0$ and the edge angle $= \pi/4$ is shown in the below figure. The pressure distribution p_r obtained by the slip line field may be utilized also for the same geometric condition of axial symmetry in a meridional plane. Total load acting on the rim tip is evaluated by

$$P_r = \pm 2\pi \int_{R_0}^{R_0 \pm r} p_r \cdot r \cdot dr, \tag{6.25}$$

where minus sign applies to the case when rim corner is filled with centripetal flow of the material.

When a material-flow into the rim ceases in a practical sence except slight increase in the filling of the cavity corner, there takes place the severely concentrated shearing deformation at the boundary 25 of Fig. 25 (b). In this final stage, upset-extrusion, the excess material is extruded into the flash with the velocity

$$\alpha = v_F/v_A = \frac{\{1 + (A/h)\}\{1 \pm A/2R)\}v_S}{(1 \pm A/R)(1 - H/h)v_A} \tag{6.26}$$

by a rapidly increasing load. If W is nearly equal to zero, this increase of load

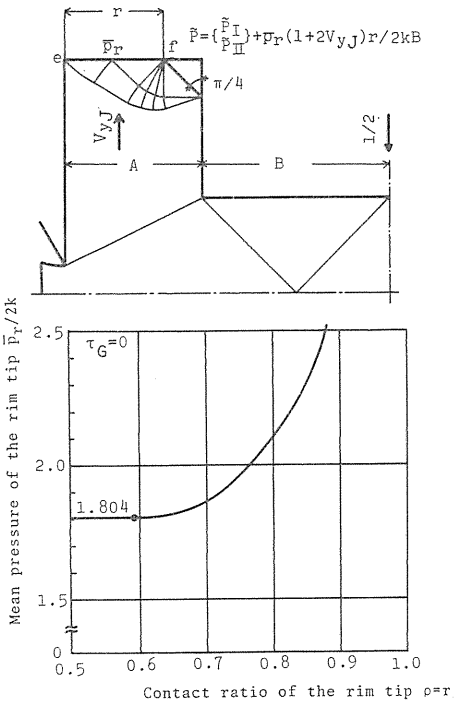

FIG. 31. Velocity field in the stage I' and variation of mean pressure of the rim tip with r/A ratio.

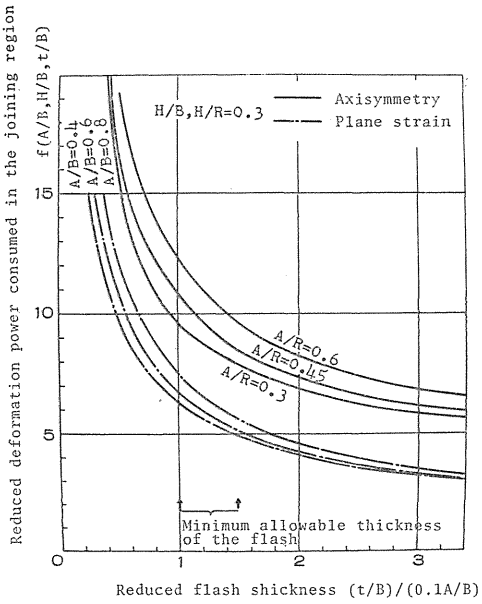

FIG. 32. Theoretical deformation power in upset-extrusion stage which is consumed in the joining region as function of reduced flash heights.

mainly comes from the increase of the specific workdone $f(A/R, H/h, A/B)$ in the joining region. Fig. 32 shows an example of the relation between f and $\{(h-H)/B\}/(0.1\cdot A/B)$ or $t/(0.1\cdot A)$. As will be seen in the figure, f increases with the decrease of the flash height, especially when $t/(0.1\cdot A)\lesssim 1$. (6.27)

In addition, upset-extrusion load P_{III} includes the effect of the rapid increase of W/t as well as f. Therefore, it is important to suppress the increase of $\tilde{P}_{III}$ by means of adjusting the dimension of the sunken depth H or of making final thickness of the flash not too thin which limitations are given by Eq. 6.27.

Let the power of deformation in stage I', II' and III be designated by $\dot{E}_I$, $\dot{E}_{II}$, and $\dot{E}_{III}$ respectively, the critical condition F, transition from I' or II' to III, should be derived from the conditions,

$$\dot{E}_{I' \text{ or } II}=\dot{E}_{III} \quad \text{or} \quad \tilde{P}_{I' \text{ or } II'}=\tilde{P}_{III}. \tag{6.28}$$

Assuming that $W=0$ in plane strain, the condition being satisfied at the critical point F can be simply written as follows.

$$\{1+(B/A)(H/h)\}[\rho(A/B)\{p_r/(2k)+q/(2B)\}]+(A^2+H^2)/(2hA)-f=0 \tag{6.29}$$

From this relation, a plot of the contact ratio of the rim tip $\rho=r/A$ as a function of the flash thickness $t/B(=(h-H/B))$ is obtained which is shown in Fig. 33. The values ρ increase with a decrease of the flash height t/B. If $t/B=(h-H)/B=$

0.08, ρ can reach above 90% even in a high wall friction of $q/B=1$ and in a small H/B. It will be concluded that the optimum final flash thickness t_1/B and optimum sunken depth H_{opt} may be determined by the condition that ρ reaches above a certain intended value.

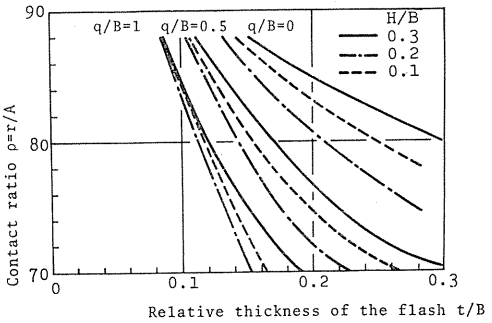

FIG. 33. Interrelation between the contact ratio of the rim tip ρ and the relative thickness of the flash t/B at the critical point F.

6.2. *Estimation of the surplus material of the blank*

The sequence of deformation modes and the critical condition C, R and F have been referred to based on the velocity fields applied in Fig. 25 and on the experimental results. By taking account of the change of α during a process and amount of the necessary boosting pressure at the critical points C and R, V_f and V_R will be estimated by the following equations.

$$\varphi=\varphi_C\left(\frac{h}{A}=\frac{h_C}{A}\right)+\left[\frac{\partial\varphi_C}{\partial(h/A)}\right]_{h/A=h_C/A}\cdot\left[\left(\frac{h}{A}-\frac{h_C}{A}\right)+\frac{(h/A-h_C/A)^2}{2(h_C/A-h_R/A)}\right] \tag{6.30}$$

$$\varphi_C=(B/b_0)\cdot\alpha_C\cdot G\cdot(R+R_1)/(r_0+R_1)\,;\quad (\alpha_C=1 \text{ and } (R+R_1)/(r_0+R_1)=1 \text{ for plane strain.}) \tag{6.31}$$

where $\alpha=\text{constant}=\alpha_C$ in cutting stage and curve ϕ in boosting stage is approximated by a quadratic equation of h/A for the simplicity's sake. If the web thickness of material at the critical points C and R are denoted by h_C and h_R, respectively, they may be given for the various conditions by

a) material which have flown into gutter at the critical point C

$$\frac{h_C}{A}=\frac{\Delta}{2}-\frac{\bar{p}_J}{k}+\frac{H}{2A}+\sqrt{\left(\frac{\Delta}{2}-\frac{\bar{p}_J}{k}+\frac{H}{2A}\right)^2-\frac{2H}{A}\left(\frac{\Delta}{2}-\frac{\bar{p}_J}{k}\right)+2\left(\frac{\tau_F W}{kA}\right)} \tag{6.32}$$

$$\frac{h_R}{A}=\frac{1}{4}\left[2\Delta-\frac{\bar{p}_J}{k}+\frac{2H}{A}+\sqrt{\left(2\Delta-\frac{p_J}{k}+\frac{2H}{A}\right)^2-\frac{8H}{A}\left(2\Delta-\frac{p_J}{k}\right)+8\left(\frac{\tau_F\cdot W}{k\cdot A}\right)}\right], \tag{6.33}$$

b) material flown into gutter before the critical point R but not at the critical point C

$$\frac{h_C}{A}=2\left\{(\tau_F/k)\frac{w_C}{t_C}+\frac{\Delta}{2}-(\bar{p}_J/k)\right\},\quad w_C=\pm\{\sqrt{R^2\pm\varphi_C V_0/(\pi t_C)}-R_0\}, \tag{6.34}$$

$$\frac{h_R}{A}=\text{Eq. 6.33},$$

c) material flown into gutter after the critical point R

$$\frac{h_C}{A}=\text{Eq. 6.32},$$

$$\frac{h_R}{A}=0.5\left\{(\tau_F/k)\frac{w_R}{t_C}+2\Delta-(p_J/k)\right\},\quad w_R=\pm\{\sqrt{R_0^2\pm\varphi_R V_0/(\pi t_R)}-R_0\}. \tag{6.35}$$

Comparison of the experimental and calculated $\phi - h/A$ curves is shown in Fig. 34 (a) and (b). Their agreement is good so that the Eqs. 6.30 and 6.31 can be applicable to find the actual volume flowing into the flash. Thus, having recourse to these equations, once the dimensions of the tool has been determined, the surplus material to be added to the blank volume or necessary volume to fill up the die can be determined.

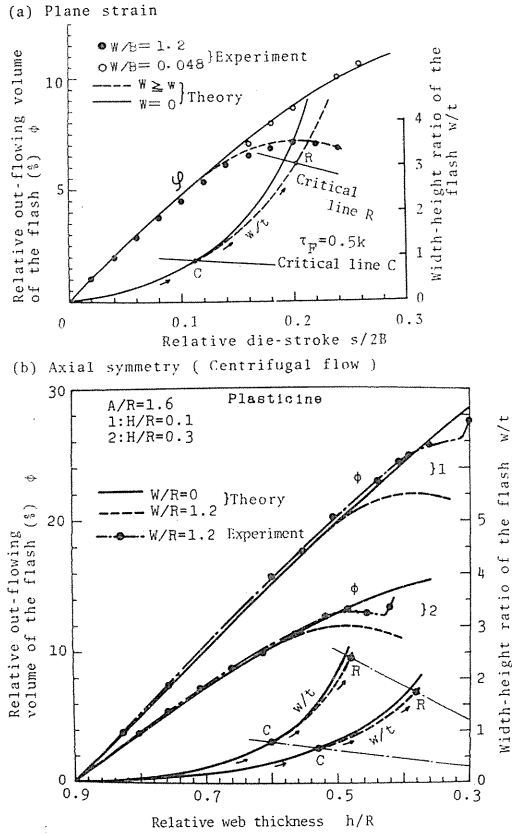

FIG. 34. Comparison of experimental and calculated relative out-flowing volume of the flash.

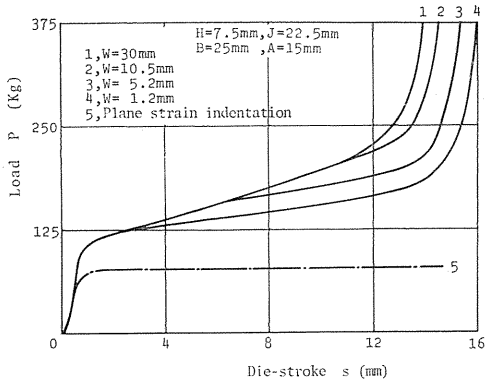

FIG. 35. Load-stroke curves of a plasticine model material.

6.3. *Load characteristics in the deformation*

In this section, the upper-bound load calculated will be examined by the measured load with plasticine material. The experiments were carried out under the conditions of controlled temperature and speed. Tool surfaces were fully lubricated by vaseline prior to the test. Examples of the experimental load-stroke curves are shown in Fig. 35 where the standard blanks listed in Table 1 have been shaped by the tools of fundamental form whose W is altered. The lowest curve 5 shows the load under a simple plane strain indentation of the web face which corresponds to the load $P_{BO}=4Bk$. Hereafter, any forming load P will be divided by P_{BO}, and the load will be examined in terms of $\tilde{P}=P/P_{BO}$.

Theoretical and experimental reduced load for several testing conditions are shown in Fig. 36. In (a) of the figure the frictional shear stress τ_F and τ_G were adequately assumed in a certain range. The experimental results show good agreement with the upper bound load, when $\tau_G=(0\sim0.1)k$ and $\tau_F=(0.5\sim0.25)k$ are assumed. The effects of W, H and h_0 on $\tilde{P}$ are seen in (b) and (c). It may be noted that in all cases the forming resistances increase markedly after

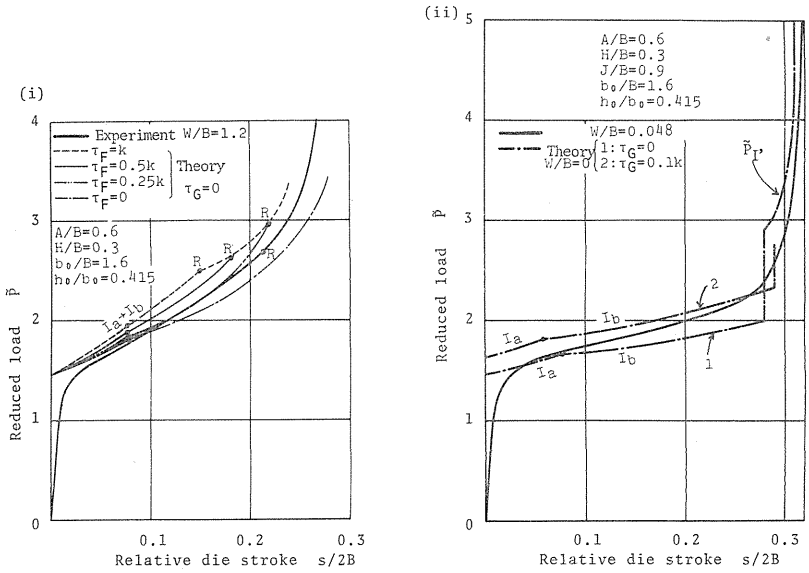

FIG. 36 (a). Reduced load: (i) Estimation of the frictional shear stress on the flash land. (ii) Estimation of the frictional shear stress on engraving surface.

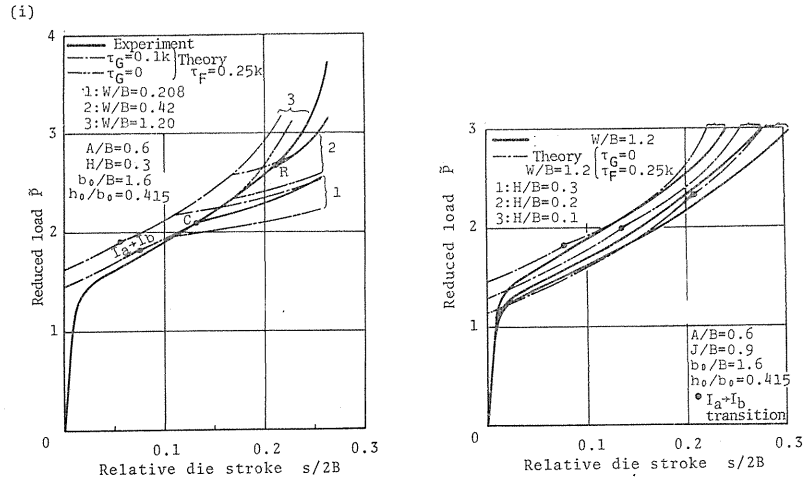

FIG. 36 (b). Reduced load: (i) Effect of the flash land width W. (ii) Effect of the sunken depth H.

the critical points R and F. Caution must be exercised for an soaring of $\overline{P}$ due to an increase of W/t and extrusion work into flash after the point F. See Fig. 37.

Deformation after the points R and F means an unnecessary energy loss. Since $\tilde{P}_{\mathrm{III}}$ must not exceed the load capacity of the machines, W should be so chosen that material can freed from the flash land prohibiting the reverse flow so to make R to come just before F.

6.4. *An approach to the optimization of forging parameters*

So far, on the basis of the theoretical and experimental considerations the mechanism of a rim or boss formation under the plane strain and the axi-symmetric conditions has been clarified fully. It has been stated that in order to improve the die-filling it is important to control the sequence of the deformation modes. And it has been also found that the forging parameters controlling this sequence are the sunken depth of the web H, the width-thickness ratio of the flash w/t or W/t and the ratio of the overhanging width to height of blank a_0/h_0 or a_0/A. The critical points of the deformation, O_s, R, F and the final load P_{III} should be noticed to optimize the forging process. Now, we shall explain how to determine these forging parameters.

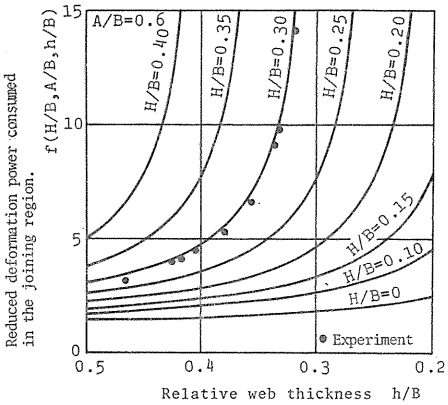

FIG. 37. Comparison of experimental and calculated upset-extrusion load $\tilde{P}_{III}=1+f$ for $W=0$.

First, the two demensional forgings having an H-shaped section with $A/B=0.6$ will be considered. The finished web height h_1 and total rim height j_1 of the forgings are assumed to be given as well as A and B. Then, the problem is how to determine the die-dimension H, W and the surplus material of blank and its width-height ratio.

Fig. 38 shows the dependence of the sunken depth H on $\tilde{P}_{III}$, j_1/A and ρ at the critical point F. If $\tilde{P}_{III}$ is limited within a certain value, for example $\tilde{P}_{III}\leqq 8$, maximum allowable H/B will be given by the abscissa of the point (i) for $\tilde{P}_{III}=8$. Since a_0/A may be defined to 1/2 according to Fig. 14 and Eq. 6.10, j_1/A can be obtained by Eq. 6.30. The results can be plotted by broken lines for the various volumes of blank as shown in the figure. When the critical conditions for R and F are simultaneously satisfied at $h=h_1=h_R$ for $\tau_F=0.5k$ and $\tau_G=0$, j_1/A can increase by the boosting action of the flash. Solid lines in Fig. 38 above show this result using the Eq. 6.31 for $h_1/B=0.32$. On the other hand it can be expected that ρ reaches above 90% even in the case of the high wall friction if $(h_1-H)/B\leqq 0.08$. Consequently, optimum sunken depth of this case may be given by $H_{opt}/B=0.26$. The relations between h_1/B, H_{opt}/B and j_1/A obtained by this way are shown in Fig. 39 where $A/B=0.6$, $a_0/A=0.5$ and $\tilde{P}_{III}=8$ were assumed. H_{opt}/B in the figure was given by $h_1/B-0.1\,A/B$. Since the point (iii) for desired j_1/A lies on one of the famiy of curves of j_1/A for constant volume of blank, the nececessary volume of blank can be found. As the volume corresponding to the solid line passing through the point (iii) is smaller than that of broken line, this possible reduction of volume will surely come from the advantage of boosting action. Especially when h_1/B is small, the surplus material of blank shows much difference according as whether the boosting stage of deformation is utilized or not.

Finally flash width W is determined by substituting $t=t_1=h_1-H$ and $h=h_2$ into the Eq. 6.24.

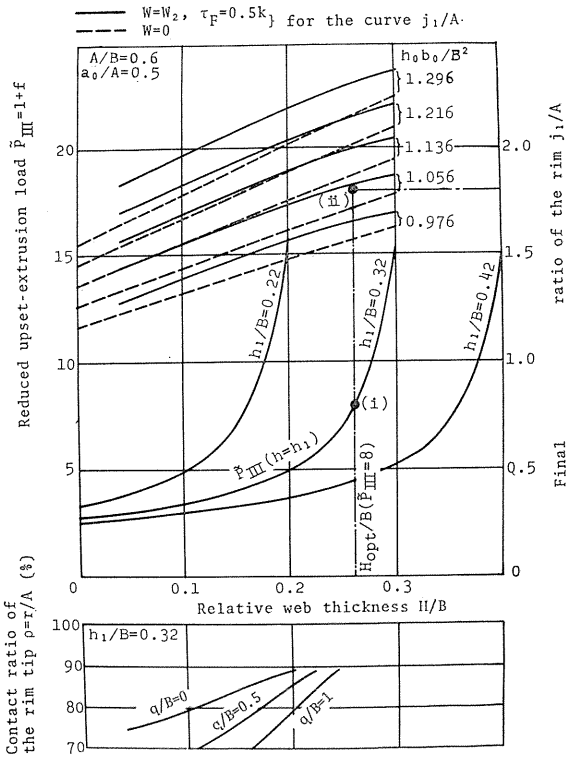

FIG. 38. Determination of the optimum sunken depth ($W_2=w_R$: See Eq. 6.35).

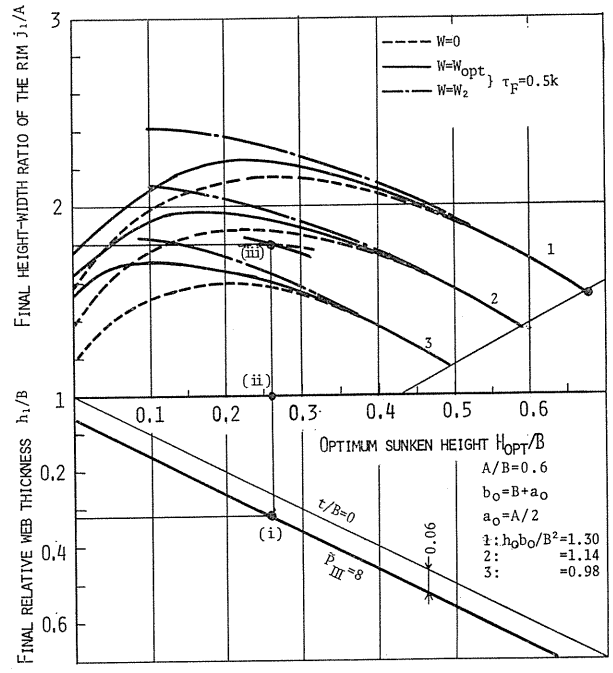

FIG. 39. Interrelation between the final width-height ratio of the rim and the optimum values of forging parameters.

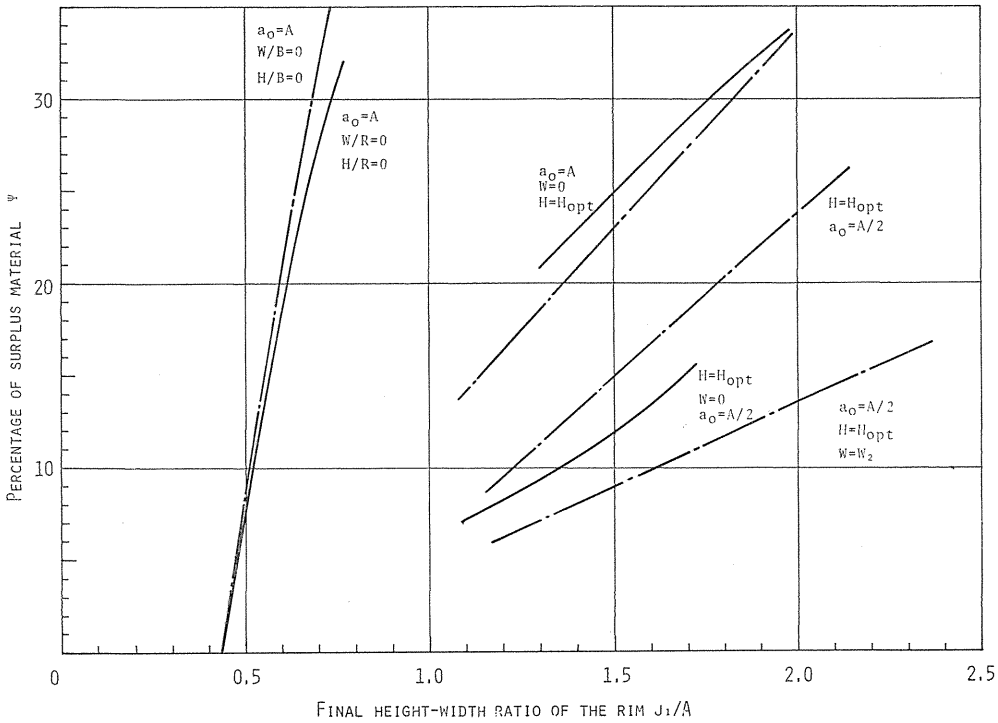

FIG. 40. Final height-width ratio of the rim obtained by optimum condition of forging parameters.
—·— Plane strain, —— Axial symmetry (Centrifugal flow)

It can clearly be seen from Fig. 40 that surplus material of the blank is able to decrease as the forging parameters H, a_0/A and W approach to their optimum values. It will be also found that optimization of H has an effect of improving the die filling both in axi-symmetric and plane strain conditions. In addition, in plane strain ψ decreases further by utilizing the boosting action of the flash. On the other hand, in axial symmetry it will be important to decrease a_0/A as possible within $a_0/h_0 \geqq 1/4$ because in general the boosting action of the flash can be expected in an axi-symmetric deformation.

7. Conclusions

Plasticine model material has been deformed by the model dies composing vertical and horizontal passages. The process of die-filling and the flow pattern of material under the plane strain and axi-symmetric conditions have been clarified fully. The results obtained are summerized as follows:

1. Material flow in the rim or boss formation can be classified into several typical modes of deformation corresponding to the geometrical condtions which are made up by die passages and filling-in material, and in a process, there appear these deformation modes in sequence. The typical modes which were noticed in this experiment are "free upsetting", "cutting", "brake-boosting", "reverse-boosting" and "upset-extrusion". These five typical modes are regarded

as prototyes of the deformation pattern for rib and boss formation under the plane strain and the axi-symmetric conditions. Individual deformation characteristics of them and their sequence have been clarified fully in order to improve the die-filling and to find an approach to the optimum design.

2. A sequence diagram of the forging process has been proposed to know the effects of various forging parameters on die-filling simultaneously. It follows from this sequence diagram that the sunken depth of the web face H and the flash land length W have a great influence on the filling-in phenomena. And it has been also found that difference exists between the axial symmetry and the plane strain in the filling-in velocity of the rim. Determination of the forging parameters can base on controlling the occurrence of the critical points R and F.

3) The dimensional factors which relates closely to the sequence are w/t or W/t, h/A and τ_F. According to the results obtained by upper-bound method which are examined by experiment, filling of the rim begins to be acceralated when w/t comes to $(k/\tau_F)\{(h/A-\Delta)/2+(\bar{p}_J/k)\}$ and is strongly boosted due to the inverse flow from flash to the die cavity when the ratio W/t or w/t increases to above the value given by $(k/\tau_F)\{2(h/A-\Delta)+(p_J/k)\}$. Therefore, flash land width W must have an enough length to satisfy above condition in the vicinity of the final stage.

4) Sunken depth H or H/A controls the filling velocity of the rim and the development of w/t. Furthermore, contact ratio at the rim tip ρ at the critical point F and the load $\tilde{P}_{\mathrm{III}}$ depend on H/h. $\tilde{P}_{\mathrm{III}}$ increases remarkably when $H/h > 1-0.1/(h/A)$. Therefore, H should be so determined that the load $\tilde{P}_{\mathrm{III}}$ and the critical point F does not exceed an allowable limit when ρ grows to an intended degree. The following condition may be given as one of the significant ground.

$$h_1-0.15A \leqq H_{\mathrm{opt}} \leqq h_1-0.1A$$

or

$$0.1A \leqq h_1-H_{\mathrm{opt}}=t_1 \leqq 0.15A$$

(For this condition ρ 90% is satisfied.)

On the other hand, flash land length W can be determined by the condition that critical point F and R coincide. *i.e.*

$$W=\{2(h/A-\Delta)+(p_J/k)\}(k/\tau_F)\cdot t_1.$$

5) In axi-symmetric condition where the material beneath the web flow scentrifugally, J/A usually increase very slowly or even decrease from h_0/A when the condition; $H/h \geqq 1-1/\{\alpha(1+A/R)\}$ is not satisfied. And development of w/t is so slow that it is rather difficult to utilize the boosting action of the flash. In this case a_0/A as well as H/A plays an important role on improving the die-filling. If overhanging length of the blank a_0 can be decrease within $a_0/h_0 \geqq 1/4$, necessary volume of blanks can decrease promisingly.

These results obtained by plasticine model material, which have been examined by utilizing the upper bound technique, will be able to clarify also the geometry of deformation in the die forging of hardened metals or an ideally plastic metal which is thought to be exercised by a hot forging. The approach mensioned above would give a useful guide for the design of the forging including rim or boss parts which have been so far defined empirically.

8. References

1) Crawley, J. and Wills, G.," Production Forging by High Energy Rate", Advances in Machine Tool Design and Research (1966), p. 5, Pergamon Press.
2) Skeen, S. A., "High Velocity Forging", Machinery and Production Engineering **4** (1965), p. 228.
3) Noland, M. C., Gadbery, H. M. and Sneegas, E. C., "High Velocity Metalworking", NASA SP-5062 (1967).
4) Dietrich, R. L. and Ansel, G., "Calculation of Press Forging Presures and Application to Magnesium Forgings", Trans. A.S.M., **38** (1947), p. 709.
5) Kudo, H., "Studies on Forging and Extrusion Processes I~IV", Kokenshuho, Univ. Tokyo, **Vol. 1** (1958), p. 38.
6) Kudo, H., "An Upper-Bound Approach to Simple Axi-symmetric Closed-Die Forging", Proc. 10th Japan National Congress for Appl. Mech. (1960), p. 145.
7) Thomsen, E. G., Yang, C. T. and Kobayashi, S., "Mechanics of Plastic Deformation in Metal Processing" (1965), p. 244, Macmillan Co.
8) Kobayashi, S. and Thomsen, E. G., "Approximate Solution to a Problem of Press Forging", Trans. A.S.M.E., Series B, **81** (1959), p. 217.
9) Meyer, H., "Die Drückspannungen in der Endphase des Gesenkschmiedens", Industrie Anzeiger, 91, Jg. Nr. 32, **V. 15.** 4 (1969), S. 59.
10) Brill, K., "Anwendung von Modellwerkstoffen zur Ermittlung der geometrischen und dynamischen Versuchsgrossen bei Gesenkformen", Werkstattstechnik. 53, Jg. **Heft 10** (1963), S. 537.
11) Stöter, J., "Der Schmiedevorgang in Hammer und Press, insbesondere hinsichtlich des Steigens", Werkstattstechnik. 49, Jg. **Heft 4** (1959), S. 223.
12) Vieregge, K., "Die Gestaltung des Gratsplts am Schmiedegesenk", Indastrie Anzeiger 92, Jg. Nr. 65, **V. 7.** 8 (1970), S. 1561.
13) Vieregge, K., "Ein Beitrag zur Gestaltung des Gratspalts beim Gesenkschmieden" (1970), Westdeutcher Verlag. Köln und Opladen.
14) Takei, H., Furukawa, T. and Okumoto, Y., "An Experimental Research on Open-Die Extrusion", J. of Japan Society for Technology of Plasticity, **Vol.** 8-47 (1967), p. 140 and **Vol.** 8-82 (1967), p. 609.
15) Takahashi, H. and Murakami, T., "Effect of Tool Angle and Friction in an Open-Die Forging in Axi-Symmetry", J. of Japan Society for Technology of Plasticity, **Vol. 12**-120 (1971), p. 31.
16) Rauhaus, H., "Untersuchungen über die Entstehung von Gesenk-Schmiedefehlern", Stahl und Eisen, **70**-7 (1950), p. 253.
17) Sabroff, A. M., Boulger, F. W. and Henning, H. J., "Forging Materials and Practices" (1963), Reinhold Book Corparation.
18) Kienzle, O. and Spies, K., "Die Gestaltung der Zwischen formen für Gesenkschmedestücke", Werkstattstechnik und Machinenbau, 49, Jg. **Heft 4** (1957), S. 176.
19) The ASM Committee on Forgings, "The Design of Closed-Die Forgings", Metal Prog. **15** (1955), p. 65.
20) Welty, G. D., "Designing Light Alloy Forgings", Machinery (A), 56 (1950).
21) Spies, K., "Eine Formennordung für Gesenkschmiedestücke", Werkstattstechnik und Machinenbau, 47, Jg. **Heft 4** (1957), S. 201.
22) Gure, C., "Designing Forged Parts for High-Strength", Production Engineering, **33**-7 (1962), p. 47,
23) Heuer, P. J., "Modelverfahren fur die Umformtechnik Fliess vorgange Werkstoffkonstante, Umformbeiwert", VDI-Forschungsheft 493 Ausgabe, Band 28 (1962).
24) Burbank, F., "Forging", Machine Design 37 (1965), p. 126.
25) Noguchi, M. and Onishi, T., "A New Enclosed Die Forging", J. of Japan Society for Technology of Plasticity, **Vol.** 6-49 (1965), p. 63.

26) Altan, T., "Computer Simulation to Predict Load, Stress and Metal Flow in an axi-symmetric Closed Die Forging", Metal Forming (1971), p. 249.
27) Naujoks, W. and Fabel, D. C., "Forging Handbook" (1939), The American Society for Metals.
28) Bruchanow, A. N. und Rebelski, A. W., "Gesenkschmieden und Warmpressen" (1955), V. E. B. Verlag Technik Berlin.
29) Lange, K., "Gesenkschmieden von Stahl" (1958), Springer Verlag.
30) American Society for Metals, "Forging and Casting", Metals Handbook 5 (1970).
31) Haller, H. N., "Handbuch des Schmiedens" (1971), Carl Hanser Verlag München.
32) American Society for Metals, "Forging Design Handbook" (1972).
33) Jordan, T. F. and Thomsen, E. G., "Comparison of an Unsymmetric Slip-Line Solution in Extrusion with Experiment", J. Mech. Phys. Solids, **4** (1956), p. 184.
34) Yang, C. T. and Thomsen, E. G., "Plastic Flow in a Lead Extrusion", Trans. A.S.M.E., **75** (1953), p. 575.
35) Dodeja, L. C. and Johnson, W., "On the Multiple Hole Extrusion of Sheets of Equal Thickness, J. Mech. and Phys. Solids, **5** (1957), p. 267.
36) Bodsworth, C., Halling, J. and Barton, J. W., "The Use of Paraffin Wax as a Model Material to Simulate the Plastic Deformation of Metals", J. Iron Steel Inst., **185** (1957), p. 375.
37) Green, A. P., "The Use of Plasticine Model to Simulate the Plastic Flow of Metals, "Phil. Mag. Ser. 7, **Vol. 47** (1951), p. 365,
38) Awano, T., "The Use of Plasticine Model Material to Examine Material Flow", J. of Japan Society for Technology of Plasticity, **Vol. 1**-3 (1960), p. 203.
39) Cook, P. M., "Dependence of Mechanical Properties of Forgings on Local Strain", J. Iron Steel Inst., **179** (1955), p. 250.
40) Hill, R., "A General Method of Analysis for Metal-Working Processis", J. Mech. Phys. Solids, **11** (1963), p. 305.
41) Johnson, W. and Mellor, P. B., "Plasticity for Mechanical Engineers" (1962), p. 402, Van Nostrand.
42) Kasuga, Y., Tsutsumi, S. and Saiki, H., "Research on Material Flow in Sunken Forging-Dies. 1st Report, Geometry of Deformation in the H-Shaped Section", Trans. Japan Soc. Mech. Engrs. **Vol. 39**-320 (1973), p. 1353.
43) Kasuga, Y., Tsutsumi, S. and Saiki, H,, "Research on Material Flow in Sunken Forging-Dies. 2nd Report, Deformation Modes and its Load Characteristics", Trans. Japan Soc. Mech. Engrs, **Vol. 39**-320 (1973), p. 1366.